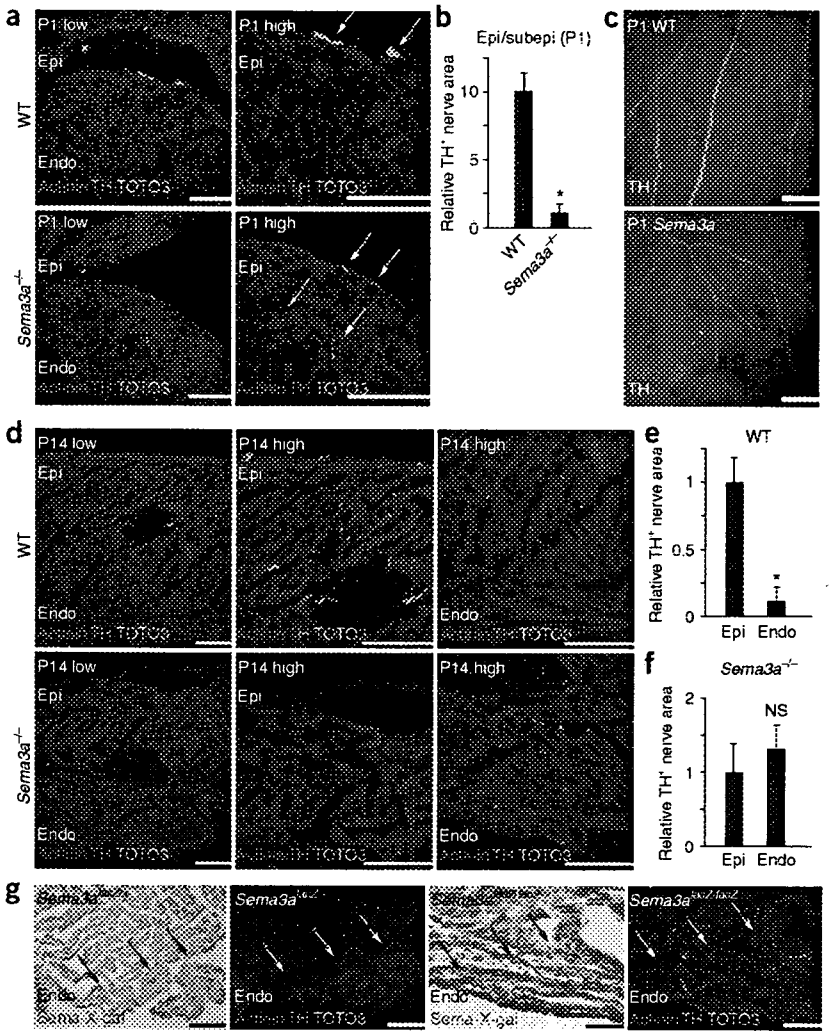

Figure 3 Cardiac sympathetic innervation patterning is disrupted in *Sema3a*-deficient mice. **(a)** Triple immunostaining for α-actinin, tyrosine hydroxylase (TH) and TOTO3 in P1 wild-type and *Sema3a*$^{-/-}$ hearts (low- and high-power fields). Arrows indicate sympathetic nerves. **(b)** Quantitative analysis of TH$^+$ nerve area in the epicardium and subepicardium in wild-type (WT) and *Sema3a*$^{-/-}$ hearts at P1 ($n = 5$). **(c)** Whole-mount immunofluorescence staining for TH in wild-type and *Sema3a*$^{-/-}$ hearts at P1. **(d)** Triple immunostaining for α-actinin, TH and TOTO3 in P14 wild-type and *Sema3a*$^{-/-}$ hearts (low- and high-power fields). An epicardial-to-endocardial gradient of sympathetic innervation was observed in wild-type hearts, but not in *Sema3a*$^{-/-}$ hearts, at P14. **(e,f)** Quantitative analysis of TH$^+$ nerve area in the subepicardium and subendocardium in wild-type and *Sema3a*$^{-/-}$ mice at P14 ($n = 5$). **(g)** Comparisons between X-gal and TH staining in P14 *Sema3a*$^{lacZ/+}$ and *Sema3a*$^{lacZ/lacZ}$ hearts are shown. Many aberrant nerves were observed in the *lacZ*-expressing area only in *Sema3a*$^{lacZ/lacZ}$ hearts (*Sema3a* homozygous null). Arrows indicate the *Sema3a*-expressing area visualized by *lacZ* expression. Representative data are shown in **a**,**c**,**d** and **g**. $^*P < 0.01$; NS, not significant. Scale bars, 100 μm.

parasympathetic activity[21,22]. The intrinsic heart rate, determined by blocking both autonomic activities, was not different between the two groups, suggesting that *Sema3a*$^{-/-}$ hearts retained intrinsic sinus node function (**Fig. 4d**). To further elucidate the autonomic activities, we performed a heart rate variability (HRV) analysis. Spectral analysis revealed a significant reduction in normalized low filtration (NLF) and in the low-to-high filtration (LF-to-HF) ratio (markers of sympathetic activity) and an increase in normalized high filtration (NHF) in *Sema3a*$^{-/-}$ mice (**Fig. 4e–g**). Thus, the intrinsic sinus node function (a cell-autonomous effect) was preserved, but sympathetic neural activity (a cell-non-autonomous effect) was significantly downregulated in *Sema3a*$^{-/-}$ hearts, presumably owing to malformation of sympathetic ganglia. These results indicated that *Sema3a*$^{-/-}$ mice develop sinus bradycardia as a result of sympathetic neural dysfunction. *Sema3a*$^{-/-}$ mice also showed spontaneous premature ventricular contractions (PVCs) (*Sema3a*$^{-/-}$: 2 of 10 mice; wild-type: 0 of 10 mice) (**Fig. 4h**). However, sustained ventricular tachycardia was not observed in either group before or after epinephrine injection.

Cardiac-specific *Sema3a* overexpression reduces innervation

It is possible that the abnormal patterning of cardiac sympathetic nerves in *Sema3a*-deficient hearts was a secondary effect of the malformation of sympathetic ganglia. To address this, we generated cardiac-specific transgenic mice expressing *Sema3a* (*SemaTG*) under the control of an α-myosin heavy chain promoter[23]. Northern blot analysis revealed that *Sema3a* was expressed exclusively in the heart. The expression of other factors known to be involved in sympathetic innervation, such as NGF and vascular endothelial growth factor-A, was unaffected in *SemaTG* mice (**Fig. 5a**). The growth cone collapse assay revealed that media conditioned with *SemaTG* cardiomyocytes had strong chemorepellent effects on sympathetic nerves, indicating that bioactive Sema3a was secreted from *SemaTG* cardiomyocytes (refs. 24,25 and **Fig. 5b**). *In situ* hybridization for *Sema3a* demonstrated *Sema3a* expression only at the subendocardium, not at the mid- or subepicardium, in wild-type hearts, similar to the results for *Sema3a*$^{lacZ/+}$ hearts. In contrast, *Sema3a* was expressed throughout the ventricles in *SemaTG* mice and showed higher expression at the subendocardium and midcardium than at the subepicardium in the ventricles. There was no *Sema3a* expression in the atrioventricular nodes or His bundles in either genotype (**Fig. 5c** and **Supplementary Fig. 3** online). Echocardiography and histology did not identify any contractile dysfunction or structural defects in *SemaTG* hearts.

To determine whether sympathetic innervation was altered in *SemaTG* mice, we immunostained mouse hearts with an antibody to tyrosine hydroxylase and measured the norepinephrine concentration in the ventricles (**Fig. 5d,e** and **Supplementary Fig. 3**). In *SemaTG* ventricles, sympathetic innervation was markedly reduced and the total cardiac norepinephrine concentration was reduced by 76%. Sympathetic innervation of the sinoatrial nodes, atrioventricular nodes and His bundles was not altered in *SemaTG* hearts (data not shown). We next analyzed the transmural difference of sympathetic innervation in *SemaTG* hearts. TH$^+$ nerve fibers and norepinephrine

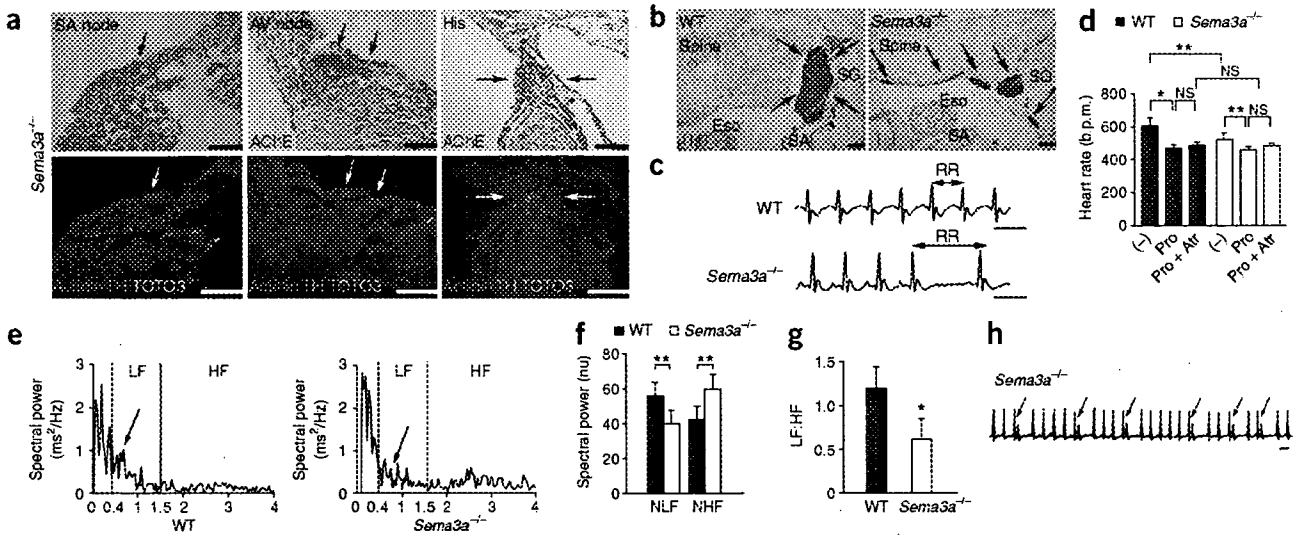

Figure 4 *Sema3a*-deficient mice display malformation of stellate ganglia and sinus bradycardia. (**a**) Top, AChE (brown) and hematoxylin (purple) staining. Bottom, immunostaining of sinoatrial node, atrioventricular node and His bundle (arrows) in P14 *Sema3a*$^{-/-}$ hearts with α-actinin, tyrosine hydroxylase (TH) and TOTO3. (**b**) Stellate ganglia (SG, arrows) in P1 animals were observed by TH immunostaining (brown). Note that a single SG was observed at a position lateral to the spine in wild-type mice, but that multiple SG were distributed widely in a dislocated pattern in *Sema3a*$^{-/-}$ mice Eso, esophagus; SA, subclavian artery. (**c**) ECG recordings from wild-type and *Sema3a*$^{-/-}$ mice. The lengthened RR interval indicates abrupt sinus slowing in *Sema3a*$^{-/-}$ mice. (**d**) Changes in heart rate following pharmacological modifications in wild-type and *Sema3a*$^{-/-}$ mice ($n = 5$). Note that propranolol reduced heart rate to a lesser extent in *Sema3a*$^{-/-}$ mice than in wild-type mice. (–), no addition; Pro, propranolol; Pro + Atr, propranolol + atropine. (**e**) Power spectra of heart-rate variability (HRV) in wild-type and *Sema3a*$^{-/-}$ mice. Note decrease of HRV across low filtration (LF) band in *Sema3a*$^{-/-}$ mice, reflecting lower sympathetic nerve activity (arrows). (**f**,**g**) The normalized low filtration (NLF) and the low-to-high filtration (LF:HF) ratio were decreased in *Sema3a*$^{-/-}$ mice ($n = 5$). (**h**) Spontaneous and frequent premature ventricular contractions (PVCs, arrows) were observed in *Sema3a*$^{-/-}$ mice. Representative data are shown in **a**–**c**, **e** and **h**. $^{*}P < 0.01$; $^{**}P < 0.05$; NS, not significant. Scale bars: 100 μm in **a**,**b**; 100 ms in **c**,**h**.

concentration were decreased proportionally at both the subepicardium and subendocardium in *SemaTG* ventricles (**Fig. 5f,g**). Therefore, sympathetic innervation density was inversely proportional to *Sema3a* expression in *SemaTG* hearts. The appearance of stellate ganglia was not different between wild-type and *SemaTG* mice (**Fig. 5h**). These results indicated that cardiomyocyte-derived Sema3a mediates repulsive and inhibitory effects on cardiac sympathetic neural growth.

SemaTG mice are susceptible to ventricular arrhythmias

The *SemaTG* mice died suddenly, without any symptoms, at 10 months of age (4 of 22 *SemaTG* mice versus 0 of 22 wild-type mice) (**Fig. 6a**), and necropsy showed no abnormalities. Telemetry ECG revealed spontaneous PVCs in *SemaTG* mice but not in wild-type mice (3 of 10 *SemaTG* mice versus 0 of 10 wild-type mice), whereas there were no significant differences in other ECG parameters (**Fig. 6b** and **Supplementary Table 2** online). Epinephrine administration induced multiple nonsustained and sustained episodes of ventricular tachycardia in the *SemaTG* mice only (2 of 10 *SemaTG* mice versus 0 of 10 wild-type mice) (**Fig. 6c**). To further characterize susceptibility to arrhythmia, we subjected wild-type and *SemaTG* mice to programmed electrical stimulation. *SemaTG* mice had nonsustained ventricular tachycardia at baseline, the frequency and duration of which were significantly increased by a low dose of isoproterenol (**Fig. 6d,e**; 8 of 10 *SemaTG* mice). In contrast, no wild-type mice ($n = 10$) developed sustained ventricular tachycardia. There were no electrophysiological differences between the two groups (**Supplementary Table 2**).

It is possible that the hypoinnervated *SemaTG* hearts showed ventricular arrhythmias as a result of catecholamine supersensitivity. To test this possibility, we measured cyclic AMP (cAMP) levels in wild-type and *SemaTG* ventricles before and after isoproterenol injection. Although basal cAMP levels were not different, the increase in cAMP after isoproterenol administration was greater in *SemaTG* mice than wild-type mice, indicating an augmented adrenergic response in *SemaTG* hearts (**Fig. 6f**). To investigate this mechanistically, we measured the density of the β_1-adrenergic receptor (β_1AR) in the ventricles. The β_1AR density was 1.5-fold greater in *SemaTG* ventricles (**Fig. 6g**).

We next investigated the transmembrane action potential of left ventricular myocytes, using glass microelectrodes. Action potential duration (APD) assessed at 50% and 90% repolarization (APD_{50} and APD_{90}) were shorter in the subepicardium than in the subendocardium in the wild-type mice. APD was significantly prolonged in hypoinnervated *SemaTG* subepicardium and subendocardium, and was inversely proportional to sympathetic innervation density. The action potential amplitude, resting membrane potential and maximum positive deflection of phase 0 upstroke were not altered, indicating that repolarization currents were disrupted in *SemaTG* hearts (**Fig. 6h**). These results suggested that the higher susceptibility of *SemaTG* mice to ventricular arrhythmia was due to catecholamine supersensitivity and APD prolongation, both of which might augment triggered activity in cardiomyocytes.

DISCUSSION

This work shows that a gradient of the neural chemorepellent Sema3a is essential for proper cardiac sympathetic innervation patterning, and that inappropriate Sema3a expression triggers various kinds of arrhythmias as a result of the disruption of this patterning. To our knowledge, this is the first identification of a critical regulatory

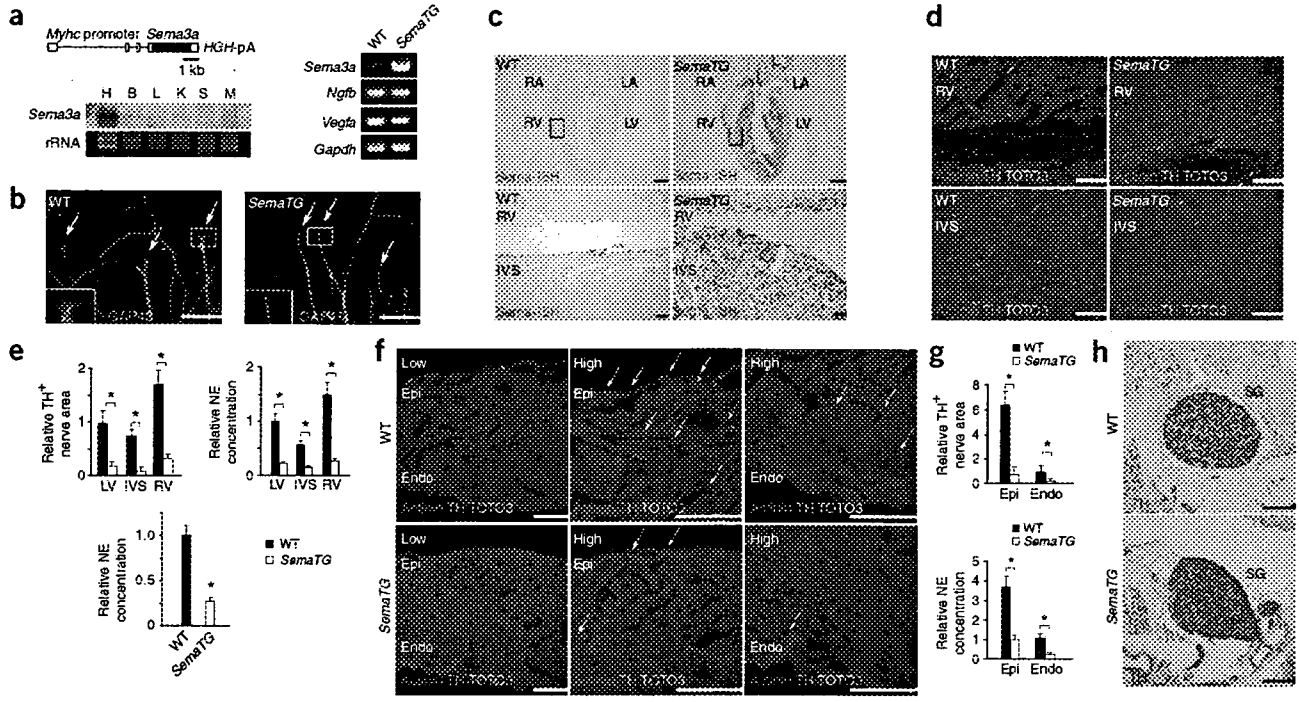

Figure 5 Cardiac sympathetic innervation patterning was disturbed in *SemaTG* hearts. (**a**) Schematic representation of the transgene containing the α-myosin heavy chain (*Myhc*) promoter, mouse *Sema3a* cDNA and human growth hormone (*HGH*) polyadenylation signal (pA). Northern blot analysis for *Sema3a* in *SemaTG* mice and RT-PCR analysis of *Sema3a*, *Ngfb*, *Vegfa* and *Gapdh* in wild-type and *SemaTG* hearts are shown. H, heart; B, brain; L, liver; K, kidney; S, spleen; M, muscle. (**b**) Growth cone collapse assay, visualized with GAP43 immunostaining. Arrows indicate growth cones. Insets show high-power views of the boxed areas. (**c**) *In situ* hybridization (ISH) for *Sema3a* in wild-type and *SemaTG* hearts. High-power views of the boxed areas are shown in the lower micrographs. (**d**) Triple immunofluorescence staining for α-actinin, tyrosine hydroxylase (TH) and TOTO3 in wild-type and *SemaTG* hearts. (**e**) TH^+ nerve areas were decreased in *SemaTG* hearts ($n = 5$). Cardiac norepinephrine (NE) concentrations were also reduced in *SemaTG* ventricles compared with wild-type ventricles ($n = 8$). (**f**) Triple immunofluorescence staining for α-actinin, TH and TOTO3 in wild-type and *SemaTG* hearts. The number of TH^+ nerves was decreased in both the subepicardium (Epi) and the subendocardium (Endo) in *SemaTG* ventricles. Arrows indicate TH^+ nerves. (**g**) Quantitative analysis of TH^+ nerve area and norepinephrine concentrations in the subepicardium and the subendocardium ($n = 5$). (**h**) Stellate ganglia (SG) were not abnormal in *SemaTG* mice. Representative data are shown in **b**–**d**,**f** and **h**. LV, left ventricle; IVS, interventricular septum; RV, right ventricle; RA, right atrium; LA, left atrium. All mice were analyzed at 6 weeks of age. * $P < 0.01$. Scale bars: 50 μm in **b**,**d**; 100 μm in lower panels of **c**; 100 μm in **f**,**h**; 1 mm in top panels of **c**.

factor for cardiac sympathetic patterning. The expression pattern of Sema3a in the heart is inversely related to sympathetic innervation. Sympathetic nerves express both the NGF receptor TrkA and the Sema3a receptor neuropilin-1 (refs. 14,24). During development, NGF and Sema3a are expressed within the spinal cord and influence pathway guidance of sensory axons. Sema3a is specifically expressed in the ventral half of the spinal cord and induces NGF-responsive sensory axons to terminate at the dorsal part of the spinal cord[13,26]. Thus, the growth cone behavior of sensory axons is modulated by coincident signaling between NGF and Sema3a (ref. 27). As cardiomyocyte-derived NGF acts as a chemoattractant and Sema3a is a potent chemorepellent for sympathetic nerves, it might be the balance between NGF and Sema3a synthesized in the heart that determines cardiac sympathetic innervation patterning. The phenotype of *Sema3a*$^{-/-}$ hearts strongly suggests that no other semaphorin ligands can compensate for loss of *Sema3* function in the control of cardiac sympathetic neural patterning.

Sema3a promotes the aggregation of neurons into sympathetic ganglia during early embryogenesis. This was demonstrated previously with displacement of sympathetic neurons and abnormal morphogenesis of the sympathetic trunk in *Sema3a*$^{-/-}$ mice observed at E12.5 (ref. 14). However, little is known about the role of Sema3a after birth. We found a sustained deficiency in sympathetic neural patterning in *Sema3a*$^{-/-}$ hearts and dislocation of stellate ganglia at P1 and P42. Sympathetic nerve density was inversely proportional to Sema3a expression in *SemaTG* hearts, in which Sema3a is expressed mainly after birth. These results indicate that endogenous Sema3a is crucial for the cardiac sympathetic patterning, not only during embryonic development but also after birth.

Sympathetic nerves modulate the function of ion channels and trigger various types of arrhythmias in diseased hearts[28,29]. However, the relationship between sympathetic innervation and arrhythmogenicity in structurally normal hearts remains unclear. *Sema3a*$^{-/-}$ mice exhibited sinus bradycardia, abrupt sinus slowing and stellate ganglia defects. Pharmacological and HRV analysis confirmed a reduced sympathetic nerve activity in *Sema3a*$^{-/-}$ hearts. Consistent with our results, right stellectomy induces sinus bradycardia and sudden, asystolic death in dogs[30,31]. *SemaTG* hearts were also highly susceptible to ventricular arrhythmias, although without contractile dysfunction or structural defects. Given that catecholamine augments systolic function, it is surprising that *SemaTG* hearts showed normal cardiac function. However, consistent with our results, patients who underwent heart transplantation and had denervated hearts did not show heart failure, whereas about 10% of the patients developed sudden

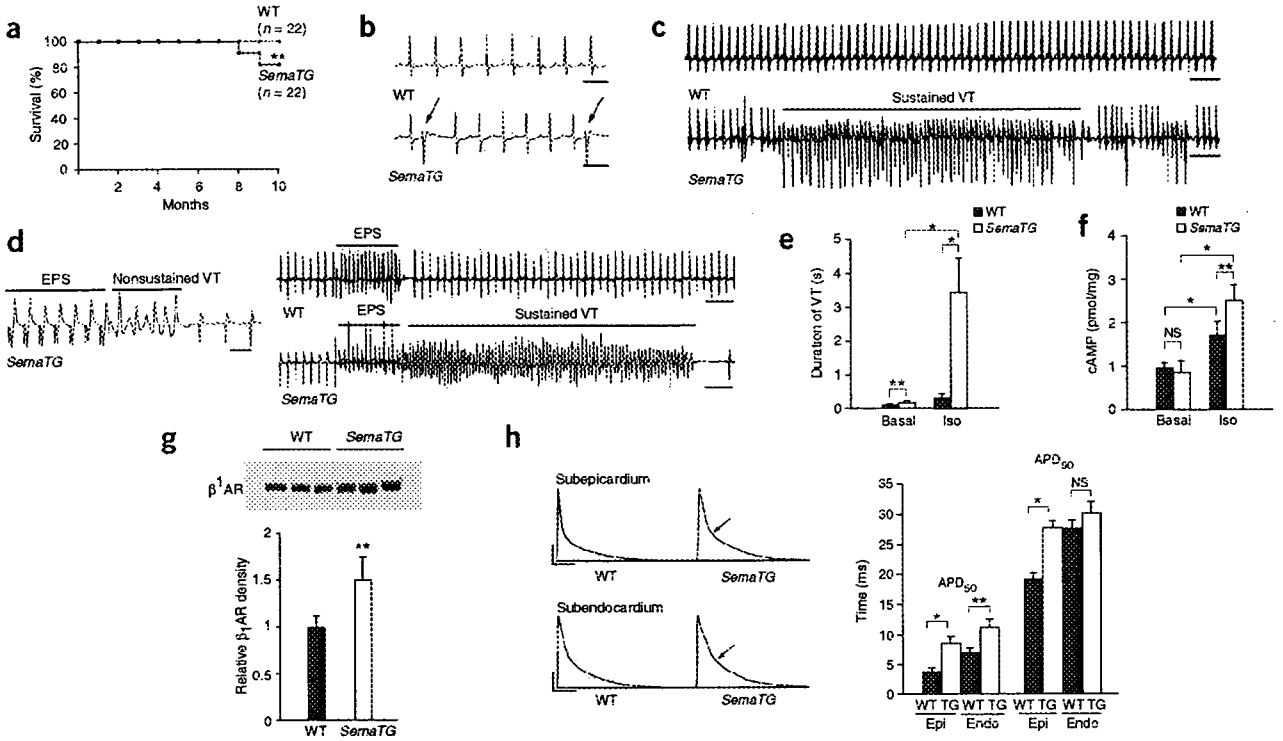

Figure 6 *SemaTG* mice are highly susceptible to induction of ventricular arrhythmia. **(a)** Survival curves of wild-type and *SemaTG* mice. **(b)** Spontaneous PVCs (arrows) were frequently observed in *SemaTG* mice. **(c)** Epinephrine administration revealed sustained ventricular tachycardia (VT) only in *SemaTG* mice. **(d)** Surface ECG during programmed electrical stimulation (EPS) showing nonsustained VT at baseline, and sustained VT after administration of isoproterenol in *SemaTG* mice. The heart was paced epicardially at an S1-S1 interval of 80 ms, followed by a premature beat of 50 ms at an S1-S2 interval. **(e)** Average duration of VT episodes before and after isoproterenol (Iso) ($n = 10$). **(f)** Intracellular concentration of cAMP at basal levels and after isoproterenol administration in wild-type and *SemaTG* hearts ($n = 5$). **(g)** Immunoblotting showed increased β_1AR levels in membrane fractions from *SemaTG* hearts. The relative β_1AR density is shown ($n = 5$). **(h)** Representative action potential tracing from wild-type and *SemaTG* subepicardium (Epi) and subendocardium (Endo). *SemaTG* subepicardium and subendocardium showed prolonged action potentials (arrows). Mean APD measured at 50% and 90% repolarization in wild-type and *SemaTG* (TG) hearts is shown (APD_{50} and APD_{90}; $n = 10$). Representative data are shown in **b–d,g** and **h**. Mice were analyzed at 6 to 8 weeks of age (**b–h**). $^*P < 0.01$; $^{**}P < 0.05$; NS, not significant. Scale bars: 20 ms and 20 mV in **h**; 100 ms in **b** and left panel of **d**; 500 ms in **c** and right panel of **d**.

cardiac death, presumably due to arrhythmias[32]. We also observed similar basal cAMP levels and upregulation of β_1AR in *SemaTG* hearts compared with wild-type hearts. These data therefore strongly support the idea that sympathetic nerves contribute to the fine control of cardiac performance on demand, but not to basal cardiac function. The findings that both the induction of ventricular tachycardia and the production of cAMP were enhanced by isoproterenol, and that *SemaTG* hearts were severely hypoinnervated, implicate adrenergic denervation supersensitivity as a cause of arrhythmogenicity in *SemaTG* mice. It is possible that Sema3a acts directly on cardiomyocytes, but we consider this unlikely, as its receptor neuropilin-1 is expressed in cardiomyocytes only at low levels[33,34]. Action potential duration was inversely proportional to sympathetic innervation density in wild-type and *SemaTG* ventricles, suggesting that sympathetic innervation might regulate repolarization currents. Given that the electrical properties of ventricular myocytes are heterogeneous and that the cardiac repolarization gradient is highly organized through a transmural structure in ventricles[35–37], it would be intriguing to investigate the relationship between sympathetic innervation patterning and the ventricular repolarization gradient.

In conclusion, our results indicate that normal sympathetic innervation patterning mediated by Sema3a is important for the maintenance of arrhythmia-free hearts. Knowledge of the mechanisms regulating sympathetic patterning in hearts may represent a new step toward potential therapies for lethal arrhythmia.

METHODS

Animals. *Sema3a*$^{-/-}$ mice and *Sema3a* knocked-in *lacZ* mice were generated as described previously[16].

Generation of transgenic mice expressing *Sema3a* in the heart. The *Sema3a* cDNA was subcloned into an expression vector containing the α-myosin heavy chain promoter[23]. Pronuclear microinjection and other procedures were performed according to standard protocols of the Keio University Animal Care Center. The transgene was identified by PCR analysis (forward primer, 5′-GTGGTCCACATTCTTCAGGA-3′; reverse primer, 5′-GAGGCAGTCAG TAGTTTGGG-3′). All mice used in this study (*Sema3a*$^{-/-}$, *Sema3a*$^{lacZ/lacZ}$ and *SemaTG*) were backcrossed ten times into the C57BL/6 background. The Keio University Ethics Committee for Animal Experiments approved all experiments in this study.

Northern blot and quantitative RT-PCR. RNA was isolated from several tissues and from left ventricular subepicardial and subendocardial sections. For northern blot analysis, 20 μg of total RNA was used. The *Sema3a* cDNA was obtained from a C57BL/6 adult brain cDNA library as described previously[11]. Quantitative RT-PCR was performed with TaqMan probes (Applied Biosystems): *Sema3a* (Mm00436469_m1) and *Vegfa* (Mm00437304_m1). The

primers and probes for *Ngfb* were as described previously[11]. The mRNA levels were normalized by comparison to *Gapdh* mRNA.

Western blot analysis. Myocardial membrane fractions were prepared by homogenization of hearts in ice-cold buffer as described[38]. Immunodetection was performed on membrane extracts with an antibody to β_1AR (Affinity BioReagents) as previously described[38]. After transfer to nitrocellulose membranes, the 64-kDa β_1AR protein was visualized by chemiluminescence detection (ECL, Amersham).

Detection of growth cone collapse. Stellate ganglia explants were removed from E14 embryos and cultured in medium containing 10% FBS and NGF (Upstate)[39]. After 24 h incubation, the explants were cultured with cardiomyocyte-conditioned media. For detection of growth cone collapse, the cultures were immunostained with an antibody to GAP43 (Chemicon)[25]. Sema3a-Fc (R&D systems) was used as a positive control.

***In situ* hybridization.** *In situ* hybridization with digoxigenin-labeled mouse *Sema3a* antisense cRNA was performed on whole embryos and paraffin-embedded sections[14]. The bound probes were visualized with alkaline phosphatase–conjugated Fab fragment of antibody to digoxigenin (Boehringer Mannheim).

Norepinephrine measurement. Norepinephrine concentration was determined by high-performance liquid chromatography (HPLC) as described previously[11].

Immunohistochemistry of hearts. Hearts were perfused from the apex with 0.4% paraformaldehyde in phosphate-buffered saline, fixed overnight, and then embedded in optimal cutting temperature (OCT) compound and frozen in liquid nitrogen. Hearts were cut longitudinally in 5-μm sections near the central conduction system to show the four chambers. Cryostat sections were stained with antibodies to α-actinin (Sigma Aldrich), connexin40 (Chemicon) and tyrosine hydroxylase (Chemicon) to detect cardiomyocytes, Purkinje fibers and sympathetic nerve fibers, respectively. The sections were incubated with secondary antibodies conjugated with Alexa 488 or 594 (Molecular Probes) and the nuclei were stained with TOTO3 (Molecular Probes). All confocal microscopy was carried out on an LSM 510 META microscope (Carl Zeiss). In some experiments, paraffin-embedded sections were stained with an antibody to tyrosine hydroxylase. Following hybridization with the secondary antibody, sections were incubated with diaminobenzidine. Nerve density was determined as described previously[11]. Briefly, we defined an epicardial portion as an epicardial half of the ventricle and an endocardial portion as an endocardial half of the ventricle for each slide. Within each portion, the six fields that contained the most nerve fiber structures were analyzed. The nerve density was the ratio between the total area of nerves and the total myocardial area, each measured by Image J software. The data for each mouse were calculated from 30 to 40 serial sections. To determine the nerve density in the conduction system, the acetyl cholinesterase–positive or connexin40-positive demarcated areas were analyzed as above. For whole-mount immunostaining, hearts were fixed with 4% paraformaldehyde and stained with an antibody to tyrosine hydroxylase.

Histological analysis. Acetyl cholinesterase staining was performed to localize the central conduction system. For serial sections of the atrioventricular node and the His bundle, anatomical landmarks were used to help guide the decision to begin collection of the sections[18,19].

Electrocardiographic recordings. Telemetric ECG recordings were obtained from conscious adult mice using a wireless implantable transmitter manufactured by Data Sciences International. Mice were anesthetized with ketamine (30 mg/kg) and xylazine (6 mg/kg) and the transmitter was placed in the abdominal cavity. The limb leads were placed in the right arm and the left leg. After implantation of the transmitter, mice were allowed to recover for at least 72 h before data collection. The telemetry data was collected continuously for 2 d and analyzed using HEM 3.4 software (Notocord Systems). Propranolol (4 mg/kg) and atropine (1 mg/kg) were injected intraperitoneally, and changes were examined during 30 min before and after injection[21]. For catecholamine stimulation, epinephrine (2 mg/kg) was injected intraperitoneally[40].

Heart-rate variability (HRV) analysis. HRV analysis was conducted following standard guidelines as described previously[41,42]. Spectral analysis using a fast Fourier transform algorithm on sequences of 512 points was performed using the HEM 3.4 software. The area under the curve was calculated for the very-low-frequency (<0.4 Hz), low-frequency (LF: 0.4–1.5 Hz) and high-frequency (HF: 1.5–4.0 Hz) bands. Spectral variability at each bandwidth was normalized (NLF, NHF) to the total spectral area[41,42].

Electrophysiology. Mice were intubated and anesthetized with 0.5% isofluorane gas, and a surface ECG was recorded during the experiment. After midline sternotomy, a bipolar stimulating electrode was positioned on the left ventricular surface. Standard pacing protocols for electrical stimulation in mice were used[43,44]. Burst pacing and 15 rapid ventricular pacing at cycle lengths of 100 ms and 80 ms with extrastimulation were performed to determine the ventricular effective refractory period (VERP) and to induce ventricular arrhythmias (with single and double extrastimuli). If arrhythmias, such as nonsustained ventricular tachycardia (3–10 beats) or sustained ventricular tachycardia (>10 beats), were induced, the protocol was repeated to determine reproducibility. After baseline measurements were completed, isoproterenol (100 μg) was administered intraperitoneally and the protocols were repeated[43,44].

Statistical analysis. Values are presented as means ± s.e.m. Differences between groups were examined for statistical significance using Student's *t*-test or ANOVA. *P* values of < 0.05 were regarded as significant.

Other methods. Other methods are listed in the **Supplementary Methods** online.

GenBank accession number. Mouse *Sema3a*, NM_009152.

Note: Supplementary information is available on the Nature Medicine website.

ACKNOWLEDGMENTS

We are grateful to J. Robbins (Cincinnati Children's Hospital) for the expression vector containing the α-myosin heavy chain promoter. We also thank Y. Tanimoto, Y. Miyake, H. Kawaguchi, E. Kobayashi and M. Nakamura for technical assistance. We are also grateful to the members of the Fukuda laboratory for their comments on the manuscript. This study was supported in part by research grants from the Ministry of Education, Culture, Sports, Science and Technology, Japan, and the Program for Promotion of Fundamental Studies in Health Sciences of the National Institute of Biomedical Innovation.

AUTHOR CONTRIBUTIONS

M.I. designed the study, conducted all experiments, and wrote the manuscript. H.K. and K.K. conducted histochemical characterization. F.H. participated in subcloning. Y.I. conducted the growth cone collapse assay. M.T. provided *Sema3a*$^{-/-}$ mice and *Sema3d*$^{lacZ/lacZ}$ mice. S.M., J.-K.L and I.K participated in and provided advice on the electrophysiology. K.M. and Y.T. participated in histochemical characterization. K.S. conducted the pronuclear microinjection. S.M. and M.S. participated in northern blotting and western blotting. S.O. provided advice on the experimental design. K.F. supported financially and supervised the whole project.

COMPETING INTERESTS STATEMENT

The authors declare no competing financial interests.

Published online at http://www.nature.com/naturemedicine
Reprints and permissions information is available online at http://npg.nature.com/reprintsandpermissions

1. Crick, S.J. *et al.* Innervation of the human cardiac conduction system. A quantitative immunohistochemical and histochemical study. *Circulation* **89**, 1697–1708 (1994).
2. Randall, W.C., Szentivanyi, M., Pace, J.B., Wechsler, J.S. & Kaye, M.P. Patterns of sympathetic nerve projections onto the canine heart. *Circ. Res.* **22**, 315–323 (1968).
3. Ito, M. & Zipes, D.P. Efferent sympathetic and vagal innervation of the canine right ventricle. *Circulation* **90**, 1459–1468 (1994).
4. Crick, S.J., Sheppard, M.N., Ho, S.Y. & Anderson, R.H. Localisation and quantitation of autonomic innervation in the porcine heart I: conduction system. *J. Anat.* **195**, 341–357 (1999).
5. Chow, L.T., Chow, S.S., Anderson, R.H. & Gosling, J.A. Innervation of the human cardiac conduction system at birth. *Br. Heart J.* **69**, 430–435 (1993).

6. Hansson, M., Kjorell, U. & Forsgren, S. Increased immunoexpression of atrial natriuretic peptide in the heart conduction system of the rat after cardiac sympathectomy. *J. Mol. Cell. Cardiol.* **30**, 2047–2057 (1998).
7. Cao, J.M. *et al.* Nerve sprouting and sudden cardiac death. *Circ. Res.* **86**, 816–821 (2000).
8. Cao, J.M. *et al.* Relationship between regional cardiac hyperinnervation and ventricular arrhythmia. *Circulation* **101**, 1960–1969 (2000).
9. Opthof, T. *et al.* Dispersion of refractoriness in canine ventricular myocardium. Effects of sympathetic stimulation. *Circ. Res.* **68**, 1204–1215 (1991).
10. Priori, S.G. & Corr, P.B. Mechanisms underlying early and delayed afterdepolarizations induced by catecholamines. *Am. J. Physiol.* **258**, H1796–H1805 (1990).
11. Ieda, M. *et al.* Endothelin-1 regulates cardiac sympathetic innervation in the rodent heart by controlling nerve growth factor expression. *J. Clin. Invest.* **113**, 876–884 (2004).
12. Kuruvilla, R. *et al.* A neurotrophin signaling cascade coordinates sympathetic neuron development through differential control of TrkA trafficking and retrograde signaling. *Cell* **118**, 243–255 (2004).
13. Puschel, A.W., Adams, R.H. & Betz, H. Murine semaphorin D/collapsin is a member of a diverse gene family and creates domains inhibitory for axonal extension. *Neuron* **14**, 941–948 (1995).
14. Kawasaki, T. *et al.* Requirement of neuropilin 1-mediated Sema3A signals in patterning of the sympathetic nervous system. *Development* **129**, 671–680 (2002).
15. Tanelian, D.L., Barry, M.A., Johnston, S.A., Le, T. & Smith, G.M. Semaphorin III can repulse and inhibit adult sensory afferents *in vivo*. *Nat. Med.* **3**, 1398–1401 (1997).
16. Taniguchi, M. *et al.* Disruption of semaphorin III/D gene causes severe abnormality in peripheral nerve projection. *Neuron* **19**, 519–530 (1997).
17. Behar, O., Golden, J.A., Mashimo, H., Schoen, F.J. & Fishman, M.C. Semaphorin III is needed for normal patterning and growth of nerves, bones and heart. *Nature* **383**, 525–528 (1996).
18. Pashmforoush, M. *et al.* Nkx2–5 pathways and congenital heart disease; loss of ventricular myocyte lineage specification leads to progressive cardiomyopathy and complete heart block. *Cell* **117**, 373–386 (2004).
19. Tago, H., Kimura, H. & Maeda, T. Visualization of detailed acetylcholinesterase fiber and neuron staining in rat brain by a sensitive histochemical procedure. *J. Histochem. Cytochem.* **34**, 1431–1438 (1986).
20. Kupershmidt, S. *et al.* Replacement by homologous recombination of the minK gene with lacZ reveals restriction of minK expression to the mouse cardiac conduction system. *Circ. Res.* **84**, 146–152 (1999).
21. Shusterman, V. *et al.* Strain-specific patterns of autonomic nervous system activity and heart failure susceptibility in mice. *Am. J. Physiol. Heart Circ. Physiol.* **282**, H2076–H2083 (2002).
22. Saba, S., London, B. & Ganz, L. Autonomic blockade unmasks maturational differences in rate-dependent atrioventricular nodal conduction and facilitation in the mouse. *J. Cardiovasc. Electrophysiol.* **14**, 191–195 (2003).
23. Gulick, J., Subramaniam, A., Neumann, J. & Robbins, J. Isolation and characterization of the mouse cardiac myosin heavy chain genes. *J. Biol. Chem.* **266**, 9180–9185 (1991).
24. Kitsukawa, T. *et al.* Neuropilin-semaphorin III/D-mediated chemorepulsive signals play a crucial role in peripheral nerve projection in mice. *Neuron* **19**, 995–1005 (1997).
25. Xu, X.M. *et al.* The transmembrane protein semaphorin 6A repels embryonic sympathetic axons. *J. Neurosci.* **20**, 2638–2648 (2000).
26. Wright, D.E., White, F.A., Gerfen, R.W., Silos-Santiago, I. & Snider, W.D. The guidance molecule semaphorin III is expressed in regions of spinal cord and periphery avoided by growing sensory axons. *J. Comp. Neurol.* **361**, 321–333 (1995).
27. Tang, X.Q., Tanelian, D.L. & Smith, G.M. Semaphorin3A inhibits nerve growth factor-induced sprouting of nociceptive afferents in adult rat spinal cord. *J. Neurosci.* **24**, 819–827 (2004).
28. Dae, M.W. *et al.* Heterogeneous sympathetic innervation in German shepherd dogs with inherited ventricular arrhythmia and sudden cardiac death. *Circulation* **96**, 1337–1342 (1997).
29. Qu, J. & Robinson, R.B. Cardiac ion channel expression and regulation: the role of innervation. *J. Mol. Cell. Cardiol.* **37**, 439–448 (2004).
30. Sosunov, E.A. *et al.* Long-term electrophysiological effects of regional cardiac sympathetic denervation of the neonatal dog. *Cardiovasc. Res.* **51**, 659–669 (2001).
31. Stramba-Badiale, M., Lazzarotti, M. & Schwartz, P.J. Development of cardiac innervation, ventricular fibrillation, and sudden infant death syndrome. *Am. J. Physiol.* **263**, H1514–H1522 (1992).
32. Chantranuwat, C. *et al.* Sudden, unexpected death in cardiac transplant recipients: an autopsy study. *J. Heart Lung Transplant.* **23**, 683–689 (2004).
33. Gitler, A.D., Lu, M.M. & Epstein, J.A. PlexinD1 and semaphorin signaling are required in endothelial cells for cardiovascular development. *Dev. Cell* **7**, 107–116 (2004).
34. Gu, C. *et al.* Neuropilin-1 conveys semaphorin and VEGF signaling during neural and cardiovascular development. *Dev. Cell* **5**, 45–57 (2003).
35. Kuo, H.C. *et al.* A defect in the Kv channel-interacting protein 2 (KChIP2) gene leads to a complete loss of I(to) and confers susceptibility to ventricular tachycardia. *Cell* **107**, 801–813 (2001).
36. Brunet, S. *et al.* Heterogeneous expression of repolarizing, voltage-gated K+ currents in adult mouse ventricles. *J. Physiol. (Lond.)* **559**, 103–120 (2004).
37. Costantini, D.L. *et al.* The homeodomain transcription factor Irx5 establishes the mouse cardiac ventricular repolarization gradient. *Cell* **123**, 347–358 (2005).
38. Takahashi, T. *et al.* Increased cardiac adenylyl cyclase expression is associated with increased survival after myocardial infarction. *Circulation* **114**, 388–396 (2006).
39. Patel, T.D., Jackman, A., Rice, F.L., Kucera, J. & Snider, W.D. Development of sensory neurons in the absence of NGF/TrkA signaling *in vivo*. *Neuron* **25**, 345–357 (2000).
40. Mohler, P.J. *et al.* Ankyrin-B mutation causes type 4 long-QT cardiac arrhythmia and sudden cardiac death. *Nature* **421**, 634–639 (2003).
41. Ecker, P.M. *et al.* Effect of targeted deletions of beta1- and beta2-adrenergic-receptor subtypes on heart rate variability. *Am. J. Physiol. Heart Circ. Physiol.* **290**, H192–H199 (2006).
42. Heart rate variability: standards of measurement, physiological interpretation and clinical use. Task Force of the European Society of Cardiology and the North American Society of Pacing and Electrophysiology *Circulation* **93** 1043 1065 (1996).
43. Wehrens, X.H. *et al.* Protection from cardiac arrhythmia through ryanodine receptor-stabilizing protein calstabin2. *Science* **304**, 292–296 (2004).
44. Kannankeril, P.J. *et al.* Mice with the R176Q cardiac ryanodine receptor mutation exhibit catecholamine-induced ventricular tachycardia and cardiomyopathy. *Proc. Natl. Acad. Sci. USA* **103**, 12179–12184 (2006).

Circ J 2007; **71:** 990–992

Guidelines for Diagnosis of Takotsubo (Ampulla) Cardiomyopathy

Sachio Kawai, MD; Akira Kitabatake, MD*; Hitonobu Tomoike, MD**; Takotsubo Cardiomyopathy Study Group***

Background It is important to differentiate takotsubo cardiomyopathy from other types of transient ventricular dysfunction. These guidelines, resulting from a workshop sponsored by the Ministry of Health, Labour, and Welfare, Idiopathic Cardiomyopathy Research Committee, outline the steps necessary for diagnosis of takotsubo cardiomyopathy.

Methods and Results The survey was conducted by mailing a questionnaire to the researchers of the 203 institutions that had made presentations on this disease at scientific meetings of the Japanese Circulation Society from November 1989 to October 2002. The questionnaires were sent and collected on January 10, 2003. Based on the results of the questionnaire, the first edition of the guidelines for diagnosis of takotsubo cardiomyopathy was prepared and evaluated at the 2003 group meeting of the Research Committee. Out of 33 researchers in Japan who had published research papers on this disease, 21 responded to the request and provided their opinions. The guidelines were revised and were approved at the 2004 group meeting.

Conclusions This summary provides standard guidelines for patients with takotsubo cardiomyopathy. (*Circ J* 2007; **71:** 990–992)

Key Words: Apical ballooning; Myocardial stunning; Ventricular dysfunction

The diagnostic criteria were developed by a consensus conference initiated by the Research Committee of Idiopathic Cardiomyopathy (Dr Akira Kitabatake, Former Chief Researcher; Dr Hitonobu Tomoike, Present Chief Researcher). To reflect the opinions of physicians who had actual experience with patients with takotsubo cardiomyopathy, 203 institutions were asked to cooperate in the preparation of the guidelines. These institutions had made presentations on this disease at scientific meetings of the Japanese Circulation Society from November 1989 to October 2002. Questionnaires asked for the observed numbers of cases (by sex), disease names in Japanese, sites of abnormal ventricular wall motion, obstruction of the ventricular outflow tract, exclusion criteria, electrocardiographic findings, symptoms, triggers, biochemical markers of myocardial damage, prognosis, fatal cases, and cases with severe sequelae. Questionnaires were sent and collected on January 10, 2003. Based on the results, the first edition of the guidelines for diagnosis of takotsubo cardiomyopathy were prepared. At the 2003 group meeting of the Idiopathic Cardiomyopathy Research Committee, an evaluation was considered necessary to determine whether this disease should be treated as a distinct clinical entity. To make the proposal more effective for the diagnostic guidelines, 33 researchers in Japan who had published research papers (original articles, reviews, and case reports, in English or Japanese) on this disease were asked to check the "Guidelines for diagnosis of takotsubo cardiomyopathy, 1st edition". The contents were: disease names in Japanese, disease names in English (including those corresponding to Japanese names), should inverted takotsubo phenomenon be included in the definition, sites of ventricular contraction abnormalities (whether or not apical ballooning alone is acceptable, should takotsubo be specify only in cases with hypercontraction of the ventricular base, and should normal contraction of the ventricular base be included), and the clinical importance of coronary angiography.

Twenty-one researchers responded to the request and provided their opinions, based on which the diagnostic guideline was revised. At the 2004 group meeting of the Research Committee of Idiopathic Cardiomyopathy, the revisions were reviewed by the members, who approved them.

For the sites of ventricular contraction, many questionnaire participants stated, "only apical ballooning is necessary". Eleven participants indicated, "cardiac base has normal contraction" and "includes a transient decrease including that in the base". Therefore, "the contraction of the cardiac base is well preserved and some cases even have the tendency for hyperkinesis" was deleted from the draft. An overwhelming number of questionnaire participants (20/21) were of the opinion that the inverted takotsubo phenomenon should not be included.

There was lack of agreement on the indication for coronary angiography; 12 researchers insisted upon acute-stage angiography and 9 stated that chronic-stage angiography was acceptable. For this reason, the following statement was incorporated into section A of the exclusions: "urgent coronary angiography is desirable for imaging during the

(Received February 26, 2007; accepted March 20, 2007)

*Department of Cardiology, Juntendo University School of Medicine, Tokyo, *Former Chief Researcher, Research Committee of Idiopathic Cardiomyopathy, Professor Emeritus, Hokkaido University, Sapporo, **Present Chief Researcher, Research Committee of Idiopathic Cardiomyopathy, National Cardiovascular Center, Director General of the Hospital, Osaka, Japan*

***Members are listed in the Appendix.

Mailing address: Sachio Kawai, MD, Department of Cardiology, Juntendo University School of Medicine, 2-1-1 Hongo, Bunkyo-ku, Tokyo 113-8421, Japan. E-mail: chyabo@med.juntendo.ac.jp

Table 1 Guidelines for Diagnosis of Takotsubo (Ampulla) Cardiomyopathy

I. Definition

Takotsubo (ampulla) cardiomyopathy is a disease exhibiting an acute left ventricular apical ballooning of unknown cause. In this disease, the left ventricle takes on the shape of a "takotsubo" (Japanese octopus trap). There is nearly complete resolution of the apical akinesis in the majority of the patients within a month. The contraction abnormality occurs mainly in the left ventricle, but involvement of the right ventricle is observed in some cases. A dynamic obstruction of the left ventricular outflow tract (pressure gradient difference, acceleration of blood flow, or systolic cardiac murmurs) is also observed.

Note: There are patients, such as cerebrovascular patients, who have an apical systolic ballooning similar to that in takotsubo cardiomyopathy, but with a known cause. Such patients are diagnosed as "cerebrovascular disease with takotsubo-like myocardial dysfunction" and are differentiated from idiopathic cases.

II. Exclusion criteria

The following lesions and abnormalities from other diseases must be excluded in the diagnosis of takotsubo (ampulla) cardiomyopathy.

A. Significant organic stenosis or spasm of a coronary artery. In particular, acute myocardial infarction due to a lesion of the anterior descending branch of the left coronary artery, which perfuses an extensive territory including the left ventricular apex (An urgent coronary angiogram is desirable for imaging during the acute stage, but coronary angiography is also necessary during the chronic stage to confirm the presence or absence of a significant stenotic lesion or a lesion involved in the abnormal pattern of ventricular contraction).

B. Cerebrovascular disease

C. Pheochromocytoma

D. Viral or idiopathic myocarditis

Note: For the exclusion of coronary artery lesions, coronary angiography is required. Takotsubo-like myocardial dysfunction could occur with diseases such as cerebrovascular disease and pheochromocytoma.

III. References for diagnosis

A. Symptoms: Chest pain and dyspnea similar to those in acute coronary syndrome. Takotsubo cardiomyopathy can occur without symptoms.

B. Triggers: Emotional or physical stress may trigger takotsubo cardiomyopathy, but it can also occur without any apparent trigger.

C. Age and gender difference: Known tendency to increase in the elderly, particularly females.

D. Ventricular morphology: Apical ballooning and its rapid improvement in the ventriculogram and echocardiogram.

E. Electrocardiogram: ST segment elevations might be observed immediately after the onset. Thereafter, in a typical case, the T-wave becomes progressively more negative in multiple leads, and the QT interval prolongs. These changes improve gradually, but a negative T-wave may continue for several months. During the acute stage, abnormal Q-waves and changes in the QRS voltage might be observed.

F. Cardiac biomarkers: In a typical case, there is only modest elevations of serum levels of cardiac enzymes and troponin.

G. Myocardial radionuclear study: Abnormal findings in myocardial scintigraphy are observed in some cases.

H. Prognosis: The majority of the cases rapidly recover, but some cases suffer pulmonary edema and other sequelae or death.

acute stage, but coronary angiography is also necessary during the chronic stage to confirm the presence or absence of a significant stenotic lesion or a lesion involved in the abnormal pattern of ventricular contraction".

The following pathological conditions are of interest.

1. Onset with symptoms suspicious of acute myocardial infarction (recent increase in asymptomatic cases and cases with dyspnea at onset).
2. Apical ballooning with akinesis and basal hyperkinesis.
3. ST segment elevation in the electrocardiogram (longer duration of ST elevation than from coronary spasm), T-wave inversion (giant negative T-wave), QT prolongation, and lack of reciprocal changes.
4. Slight elevation of cardiac enzymes (low values not proportional to the hypokinetic area).
5. Lack of significant coronary artery stenosis. Low provocation rate of coronary artery spasm (approximately 1/3).
6. Rapid normalization of the abnormal pattern of ventricular contraction, the electrocardiogram, cardiac enzymes and troponin, and the myocardial scintigram.
7. Higher incidence in elderly females (7-fold that of males).
8. Trigger factor of emotional stress[1,2] (predominantly emotional stress in females and physical stress in males)
9. Presence of myocardial tissue damage. Some cases might have the sequel of ventricular aneurysm.
10. Reversible outflow tract obstruction might be observed in both ventricles.
11. Some cases may have an elevation in serum catecholamine levels.
12. The pathological conditions change and improve in response to various types of drugs: intracoronary verapamil improves coronary blood flow; intracoronary nicorandil improves ST elevation; intravenous propranolol or cibenzoline improves the outflow tract gradient and ST elevation.
13. The apical region is not opacified on contrast echocardiography.
14. There is an abnormality of coronary flow reserve in Doppler flow-wire studies.
15. In severe cases, respiratory failure can occur.
16. Fatal cases exist (eg, from cardiac rupture).

Acknowledgment

This research was supported by a granted from the Ministry of Health, Labour, and Welfare, Research Grant for Intractable Diseases, Idiopathic Cardiomyopathy Research Committee.

References

1. Owa M, Aizawa K, Urasawa N, Ichinose H, Yamamoto K, Kurasawa K, et al. Emotional stress-induced "ampulla cardiomyopathy": Discrepancy between the metabolic and sympathetic innervation imaging performed during the recovery course. *Jpn Circ J* 2001; **65**: 349–352.
2. Ueyama T, Kasamatsu K, Hano T, Yamamoto K, Tsuruo Y, Nishio I. Emotional stress induces transient left ventricular hypocontraction in the rat via activation of cardiac adrenoceptors: A possible animal model of "tako-tsubo" cardiomyopathy. *Circ J* 2002; **66**: 712–713.

Appendix 1

Ikuo Segawa (Memorial Heart Center, Second Department of Internal Medicine, Iwate Medical University), Kazuhumi Tuchihashi (Second Department of Internal Medicine, Sapporo Medical University), Hiroshi Okamoto (Department of Cardiovascular Medicine, Faculty of Medicine, Hokkaido University), Jun Sawada (Department of Internal Medicine, The Cardiovascular Institute), Morimasa Takayama (Intensive Care Unit, Nippon Medical School), Youji Ogawa (Department of Cardiology, Tokyo Women's Medical University Hospital), Akihiro Niwa (Department of Cardiology, Musashino Red Cross Hospital), Yoshihiko Miyake (St. Marianna University School of Medicine Hospital), Osamu Nakayama (International Goodwill Hospital), Takanori Yasu (Clinical Pharmacology & Therapeutics, University of The Ryukyus School of Medicine), Hiroshi Imamura (First Department of Internal Medicine, School of Medicine, Shinshu University), Mafumi Owa (Department of Cardiology, Suwa Red Cross Hospital), Kazuyuki Sakata (Department of Cardiology, Shizuoka General Hospital), Isao Morii (Division of Cardiology, National Cardiovascular Center), Yoshio Ishida (Department of Radiology and Nuclear Medicine, National Cardiovascular Center), Yoshio Kohno (Department of Cardiology, Kyoto First Red Cross Hospital), Kazuaki Mitsufuji and Kazushige Tsunoda (Department of Cardiovascular Medicine, Kurashiki Central Hospital), Satoshi Kurisu and Masaharu Ishihara (Department of Cardiology, Hiroshima City Hospital), Toshihiko Yamasa (Sasebo City General Hospital), Koushi Mawatari (Department of Cardiovascular Medicine, Kagoshima Seikyo General Hospital).

Journal of the American College of Cardiology
© 2006 by the American College of Cardiology Foundation
Published by Elsevier Inc.

Vol. 47, No. 7, 2006
ISSN 0735-1097/06/$32.00
doi:10.1016/j.jacc.2005.10.069

Prognostic Value of Pacing-Induced Mechanical Alternans in Patients With Mild-to-Moderate Idiopathic Dilated Cardiomyopathy in Sinus Rhythm

Akihiro Hirashiki, MD,*† Hideo Izawa, MD, PHD,† Fuji Somura, MD, PHD,‡ Koji Obata, PHD,* Tomoko Kato, MD, PHD,† Takao Nishizawa, MD, PHD,* Akira Yamada, MD,† Hiroyuki Asano, MD,† Satoru Ohshima, MD,† Akiko Noda, PHD,§ Shigeo Iino, MD, PHD,† Kohzo Nagata, MD, PHD,§ Kenji Okumura, MD, PHD,† Toyoaki Murohara, MD, PHD,† Mitsuhiro Yokota, MD, PHD, FACC*

Nagoya, Japan

OBJECTIVES The relation between the occurrence of pacing-induced mechanical alternans and prognosis in patients with mild-to-moderate idiopathic dilated cardiomyopathy (IDCM) in sinus rhythm was investigated prospectively. The myocardial expression of genes for Ca^{2+}-handling proteins in such patients was also examined.

BACKGROUND Mechanical alternans occurs in some patients with severe heart failure, but the relation between the occurrence of mechanical alternans and prognosis in patients with IDCM has remained unknown.

METHODS Left ventricular (LV) pressure was measured during atrial pacing, and LV endomyocardial biopsy specimens were collected in 36 IDCM patients and 8 controls. Idiopathic dilated cardiomyopathy patients were divided into two groups consisting of 22 individuals who did not develop mechanical alternans at heart rates up to 140 beats/min (group A) and of 14 individuals who did (group B). The patients were followed up for a mean of 3.7 years.

RESULTS There was no significant difference in LV ejection fraction or the plasma concentration of brain natriuretic peptide between groups A and B. The myocardial abundance of ryanodine receptor 2 messenger ribonucleic acid (mRNA) was significantly lower in groups A and B than in controls, whereas that of sarcoplasmic reticulum Ca^{2+}-ATPase mRNA was significantly lower in group B than in group A or controls. Stepwise multivariate analysis identified pacing-induced mechanical alternans as the strongest predictor of cardiac events. Event-free survival in group A was significantly greater than that in group B.

CONCLUSIONS The occurrence of pacing-induced mechanical alternans is a potentially useful indicator of poor prognosis in patients with mild-to-moderate IDCM in sinus rhythm. (J Am Coll Cardiol 2006;47:1382–9) © 2006 by the American College of Cardiology Foundation

Idiopathic dilated cardiomyopathy (IDCM) is characterized by progressive left ventricular (LV) dilation and greatly impaired LV systolic function, eventually culminating in end-stage congestive heart failure (CHF) and cardiac death (1,2). It is therefore important to identify as early as possible patients with IDCM who are unlikely to improve or stabilize in response to standard medical treatment. Several studies have attempted to find clinical or other abnormalities associated with poor prognosis in such individuals. Markers examined have included indexes related to LV systolic or diastolic function, such as LV ejection fraction (LVEF), LV end-diastolic dimensions and pressures, and the plasma concentration of brain natriuretic peptide (BNP) (2–6). However, LVEF is load-dependent, and plasma BNP level is affected by changes in LV wall stress during treatment (7–9), properties that may limit their predictive value. Furthermore, the plasma concentration of BNP has been found to be less accurate for detection of milder degrees of systolic dysfunction (10), which are more common than are severe forms but are also associated with increased risk of mortality.

Mechanical alternans has been detected in both patients with severe heart failure and animal models of this condition (11–13). Although rare under resting conditions in individuals with controlled heart failure (14), mechanical alternans is more prevalent and likely to be sustained at higher heart rates (15). The relation between the occurrence of mechanical alternans and the prognosis of patients with IDCM has not previously been examined, however.

Atrial fibrillation is common in patients with IDCM and is associated with a variety of potentially deleterious hemodynamic consequences that might exert a negative influence on prognosis and accelerate the progression of LV systolic dysfunction (16). The overall survival rate for patients in sinus rhythm is higher than that for patients with atrial fibrillation (16,17). However, prognostic indicators for pa-

From the *Department of Cardiovascular Genome Science, Nagoya University School of Medicine, Nagoya, Japan; †Department of Cardiology, Nagoya University Graduate School of Medicine, Nagoya, Japan; ‡Nagoya Ekisaikai Hospital, Nagoya, Japan; and §Nagoya University School of Health Sciences, Nagoya, Japan.

Manuscript received August 22, 2005; revised manuscript received September 29, 2005, accepted October 25, 2005.

Abbreviations and Acronyms

BNP	= brain natriuretic peptide
CHF	= congestive heart failure
GAPDH	= glyceraldehyde-3-phosphate dehydrogenase
IDCM	= idiopathic dilated cardiomyopathy
LV	= left ventricle or left ventricular
$LVdP/dt_{max}$	= maximal first derivative of LV pressure
LVEF	= left ventricular ejection fraction
mRNA	= messenger ribonucleic acid
RT-PCR	= reverse transcription-polymerase chain reaction
SERCA2	= sarcoplasmic reticulum Ca^{2+}-ATPase
$T_{1/2}$	= pressure half-time

tients with mild-to-moderate IDCM in sinus rhythm remain unclear. We have therefore now examined prospectively the prognostic value of pacing-induced mechanical alternans in patients with mild-to-moderate IDCM in sinus rhythm.

METHODS

Subjects. We studied 36 patients with mild-to-moderate IDCM (mean age, 49 years; range, 32 to 62 years), 26 of whom had previously been admitted to hospital because of heart failure with dyspnea on exertion, palpitations, or peripheral edema. The remaining 10 patients were asymptomatic and were identified on the basis of an electrocardiogram abnormality at an annual health check. The IDCM of the patients was defined as mild-to-moderate on the basis of clinical symptoms.

All patients showed a normal sinus rhythm; IDCM was defined on the basis of the presence of both a reduced LVEF (<50% as determined by contrast left ventriculography) and a dilated LV cavity in the absence of coronary or valvular heart disease, arterial hypertension, or cardiac muscle disease caused by any known systemic condition (18). None of the patients had an identifiable family history of dilated cardiomyopathy in a second-degree relative. The 26 patients who had previously been hospitalized for acute heart failure were receiving treatment and were in stable condition before their referral to Nagoya University Hospital for cardiac catheterization. The period that elapsed between hospitalization and catheterization averaged 4.0 months (range, 2 to 8 months).

The control subjects consisted of eight individuals undergoing diagnostic cardiac catheterization for evaluation of atypical chest pain and a mild ST-T abnormality on their electrocardiograms. All control subjects manifested normal echocardiograms, coronary arteriograms, and contrast ventriculograms. Endomyocardial biopsies were also performed to exclude myocarditis or specific heart muscle disease, and all control subjects had normal pathological findings. The study protocol was approved by the appropriate institutional review committee, and written informed consent was obtained from all subjects.

Cardiac catheterization. A 6-F fluid-filled pigtail catheter with a high-fidelity micromanometer (model SPC-464D, Millar Instruments, Houston, Texas) was advanced into the LV through the right femoral artery for measurement of LV pressure. A 6-F bipolar pacing catheter was introduced through the right femoral vein and positioned in the right atrium. Right atrial pacing was initiated at 80 beats/min and increased in increments of 10 beats/min. Micromanometer pressure signals and standard electrocardiograms were recorded with a multichannel recorder (MR-40, TEAC, Tokyo, Japan) throughout the procedure. Left ventricular pressure signals were digitized at 3-ms intervals and analyzed with a 32-bit microcomputer system and software developed in-house. We selected steady-state LV pressure data at the baseline and at each pacing rate for analysis. We calculated the maximal first derivative of LV pressure (LV dP/dt_{max}) as an index of contractility. To evaluate LV isovolumic relaxation, we computed the pressure half-time ($T_{1/2}$) directly as previously described (19). The peak pacing rate was defined as the heart rate at which second-degree atrioventricular block occurred. After completion of the pacing study, selective coronary angiography as well as left ventriculography was performed. Endomyocardial biopsy was also performed in all patients to exclude myocarditis or specific heart muscle disease. Several (at least three) endomyocardial biopsy specimens were obtained from the free wall of the LV. Biopsy samples for messenger ribonucleic acid (mRNA) analysis were frozen immediately in liquid nitrogen and stored at −80°C until use.

Quantitative reverse transcription-polymerase chain reaction (RT-PCR) analysis. Quantitative RT-PCR analysis of the amounts of the mRNAs for glyceraldehyde-3-phosphate dehydrogenase (GAPDH), sarcoplasmic reticulum Ca^{2+}-ATPase (SERCA2), ryanodine receptor 2, phospholamban, calsequestrin, and the Na^{+}-Ca^{2+} exchanger was performed with a Prism 7700 Sequence Detector (Perkin-Elmer, Foster City, California) as previously described (20). Variability in the efficiency of cDNA synthesis was corrected by dividing the levels of Ca^{2+}-handling protein mRNAs by that of GAPDH mRNA.

Study protocol. To evaluate whether the rate of cardiac events differed between patients with or without pacing-induced mechanical alternans, we prospectively followed up all patients for the occurrence of primary events, which were defined as cardiac death (from worsening CHF or sudden death) or the unscheduled readmission for decompensated CHF. Noncardiac death was excluded.

Statistical analysis. Data are presented as means ± SD. Baseline characteristics and hemodynamic variables were compared among groups by one-way factorial analysis of variance; if a significant difference was detected, intergroup comparisons were performed with Scheffe's multiple-comparison test. Reverse transcription-polymerase chain reaction analysis of the abundance of Ca^{2+}-handling protein mRNAs among groups were also compared by one-way

JACC Vol. 47, No. 7, 2006
April 4, 2006:1382–9

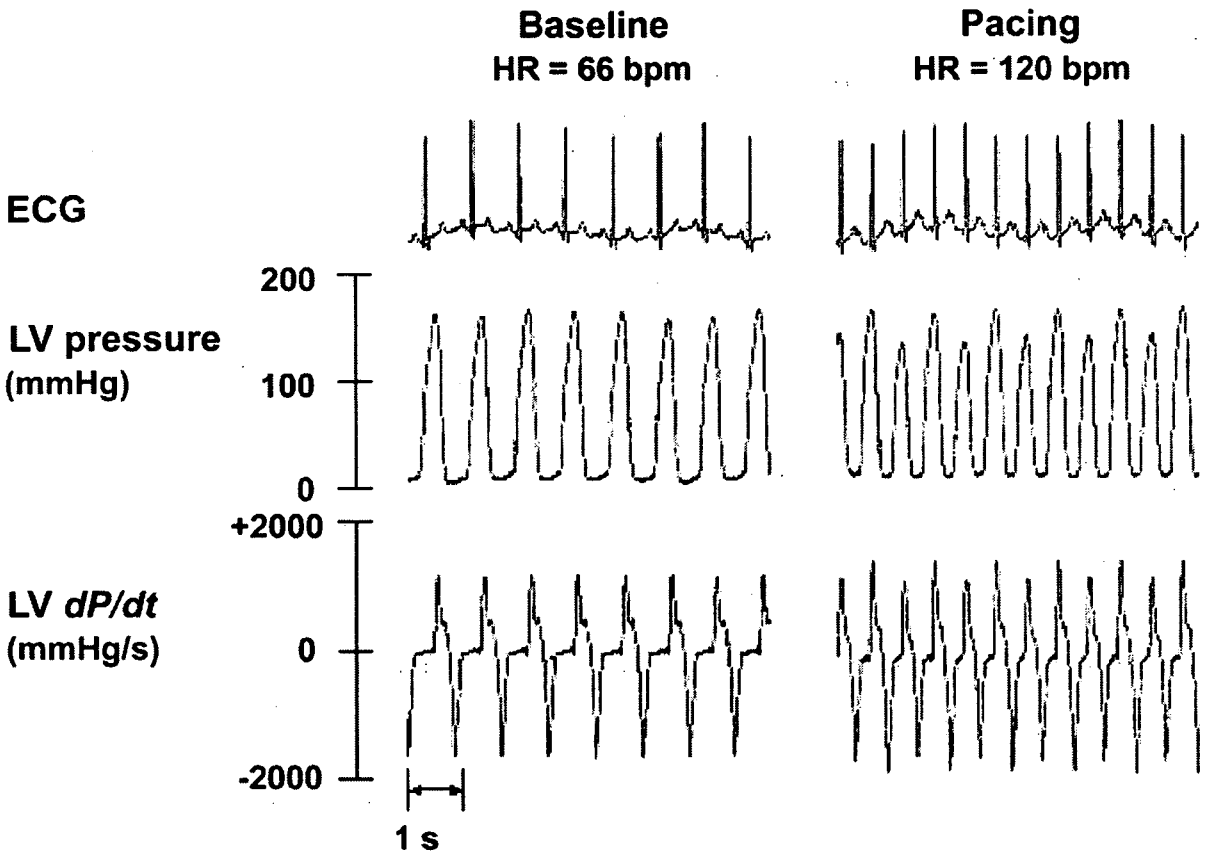

Figure 1. Representative records of pacing-induced mechanical alternans. The traces represent a lead II electrocardiogram (ECG), left ventricular (LV) pressure, and LV *dP/dt* at a baseline heart rate (HR) of 66 beats/min (bpm) and at atrial pacing of 120 bpm for a male patient with idiopathic dilated cardiomyopathy. Alternating pressure was 30 mm Hg at the pacing rate of 120 bpm. Both LV dP/dt_{max} and LV dP/dt_{min} showed alternating changes with LV pressure. dP/dt = first derivative of left ventricular pressure.

factorial analysis of variance if a significant difference was detected. Within-group comparisons for changes in hemodynamic variables between baseline and 120 beats/min of atrial pacing were performed with the paired Student *t* test. Comparisons between measurements from the strong and weak beats of mechanical alternans were also performed with the paired Student *t* test. Cox proportional hazard regression analysis was performed to identify independent predictors of cardiac events. We also performed a stepwise forward selection procedure. Cumulative cardiac event estimates were calculated by the Kaplan-Meier method; differences between the survival curves were assessed by the log-rank test. All analyses were performed with the SPSS 12.0 software package (SPSS Inc., Chicago, Illinois). A p value of <0.05 was considered statistically significant.

RESULTS

Classification of IDCM patients based on mechanical alternans. Mechanical alternans was diagnosed if the pressure difference between the strong and weak beats was ≥4 mm Hg. Under baseline conditions, no patient exhibited mechanical alternans. We divided the IDCM patients into two groups on the basis of the absence or presence of pacing-induced mechanical alternans. Group A consisted of 22 IDCM patients who did not develop mechanical alternans at heart rates up to 140 beats/min, whereas group B comprised 14 IDCM patients who did. The average heart rate at which mechanical alternans appeared (critical pacing heart rate) in IDCM patient group B was 99 ± 10 beats/min. Waveforms at baseline and 120 beats/min of pacing for a representative male IDCM patient with pacing-induced mechanical alternans are shown in Figure 1.

Baseline clinical data. Baseline clinical characteristics for the control group and IDCM patient groups A and B are shown in Table 1. There were no significant differences in age or sex among the three study groups. All IDCM patients were classified as New York Heart Association functional class I or II at the time of cardiac catheterization. Of the 36 IDCM patients, 12 had been treated previously with digitalis, 28 with diuretics, 26 with angiotensin-converting enzyme inhibitors or angiotensin-II receptor blockers, and 19 with beta-blockers. There were no signifcant differences in drug treatment at entry into the study between patient groups A and B. There was also no significant difference in LVEF between groups A and B. The LV end-diastolic and end-systolic volumes were both significantly increased in IDCM patient group B compared with those in group A. The plasma BNP level tended to be

Table 1. Baseline Clinical Characteristics

Characteristics	Controls (n = 8)	IDCM Group A (n = 22)	IDCM Group B (n = 14)
Age (yrs)	45 ± 12	48 ± 13	51 ± 12
Gender (M/F)	8/0	20/2	11/3
NYHA functional class			
I		13 (59%)	6 (43%)
II		9 (41%)	8 (57%)
Prior treatment			
Digitalis	0	6 (27%)	6 (43%)
Diuretics	0	16 (73%)	12 (86%)
ACE inhibitors or AR blockers	0	17 (77%)	9 (64%)
Beta-blockers	0	10 (45%)	9 (64%)
LV end-diastolic dimension (mm)	49 ± 5	61 ± 8*	69 ± 9*†
LV end-systolic dimension (mm)	31 ± 5	50 ± 8*	58 ± 9*†
IVS thickness (mm)	10 ± 2	9 ± 2	9 ± 1
LVPW thickness (mm)	10 ± 2	9 ± 2	9 ± 1
LV mass index (g/m^2)	131 ± 38	142 ± 57	172 ± 48
LV end-diastolic volume (ml)	133 ± 45	170 ± 59	253 ± 112*†
LV end-systolic volume (ml)	40 ± 21	108 ± 50	184 ± 90*†
LVEF (%)	66 ± 8	37 ± 9*	33 ± 8*
PAWP (mm Hg)	8 ± 3	9 ± 4	16 ± 9‡§
Cardiac index ($l\ min^{-1}\ m^{-2}$)	3.36 ± 1.41	2.93 ± 0.49	2.70 ± 0.92
Plasma BNP (pg/ml)	6 ± 3	68 ± 69	98 ± 116

*$p < 0.01$ vs. controls; †$p < 0.01$ vs. group A; ‡$p < 0.05$ vs. controls; §$p < 0.05$ vs. group A.
ACE = angiotensin-converting enzyme; AR = angiotensin-II receptor; BNP = brain natriuretic peptide; IDCM = idiopathic dilated cardiomyopathy; IVS = interventricular septum; LV = left ventricular; LVEF = LV ejection fraction; LVPW = LV posterior wall; NYHA = New York Heart Association; PAWP = pulmonary arterial wedge pressure.

higher in group B than in the control group or in group A, but these differences were not significant.

Given that 10 of the 22 patients in group A and 6 of the 14 patients in group B could not achieve a heart rate of >130 beats/min because of Wenckebach block, we compared hemodynamic variables at baseline with those at 120 beats/min of pacing (Table 2). There was no significant difference in LV peak-systolic pressure or LV end-diastolic pressure at baseline among the three groups of subjects; IDCM patients exhibited a lower LV dP/dt_{max} and a longer $T_{1/2}$ than did controls at baseline. There was no significant difference in LV dP/dt_{max} or $T_{1/2}$ between patient groups A and B at baseline.

Abundance of Ca^{2+}-handling protein mRNAs in endomyocardial biopsy specimens. The amounts of Ca^{2+}-handling protein mRNAs in endomyocardial biopsy specimens were determined by RT-PCR analysis and were normalized relative to that of GAPDH mRNA (Table 3). The abundance of SERCA2 mRNA in the LV myocardium was significantly reduced in patient group B compared with that in patient group A or in the control group. The amount of ryanodine receptor 2 mRNA was significantly reduced in patient groups A and B compared with that in the control group. No significant differences in the levels of phospholamban, calsequestrin, or Na^+-Ca^{2+} exchanger mRNAs or in the SERCA2/Na^+-Ca^{2+} exchanger mRNA ratio were apparent among the three groups.

Univariate and multivariate analysis of cardiac events. Univariate analysis revealed that pacing-induced mechanical alternans, heart rate, LV end-diastolic pressure, the ratio of LV end-diastolic pressure to cardiac index, and LVEF were significant predictors of cardiac events (Table 4). These variables were then subjected to stepwise multivariate analysis, yielding only pacing-induced mechanical alternans as a significant independent predictor of cardiac events.

Event-free survival. The cumulative probability of event-free survival was calculated by the Kaplan-Meier method (Fig. 2). All patients with IDCM were followed for an average of 3.7 years (range, 0.8 to 7.5 years) starting at the time of catheterization and ending with a cardiac event or the most recent evaluation of survivors. Two patients (one in each of groups A and B) were excluded from this analysis because they died of noncardiac causes. Cardiac death occurred in one patient in group A and two patients in group B. One patient in group A experienced CHF. Six patients in group B experienced cardiac events, classified as CHF in five and syncope in one. The three-year cumulative probabilities of event-free survival were 88.1% in group A and 40.4% in group B. The probability of event-free survival in group A was significantly higher than that in group B by the log-rank test.

DISCUSSION

We have shown that the occurrence of pacing-induced mechanical alternans was a predictor of poor prognosis in patients with mild-to-moderate IDCM in sinus rhythm, and that the abundance of SERCA2 mRNA in LV endo-

Table 2. Hemodynamic Variables at Baseline and at a Heart Rate of 120 Beats/min During Pacing

Variables	Baseline	Pacing	p Value
Heart rate (beats/min)			
Controls	62 ± 6	120 ± 0	
Group A	70 ± 12 * †	120 ± 0	
Group B	90 ± 18	120 ± 0	
LVPSP (mm Hg)			
Controls	124 ± 27	119 ± 16	
Group A	121 ± 18	118 ± 18	
Group B	119 ± 20	117 ± 21 (strong) ‡	
		109 ± 20 (weak)	§
LVEDP (mm Hg)			
Controls	9 ± 4	3 ± 3	§
Group A	11 ± 7	7 ± 7	§
Group B	16 ± 10	13 ± 9 (strong) ‡	§
		11 ± 9 (weak)	§
LV dP/dt_{max} (mm Hg/s)			
Controls	1,759 ± 361	2,131 ± 487	§
Group A	1,275 ± 246 *	1,411 ± 275 *	§
Group B	1,145 ± 237 *	1,291 ± 264 (strong) ‡ ‖	§
		1,148 ± 225 (weak)	§
$T_{1/2}$ (ms)			
Controls	31 ± 2	25 ± 3	
	¶ ¶	¶ ¶ ¶	
Group A	41 ± 9	35 ± 8	§
Group B	42 ± 8	36 ± 8 (strong) ‡	§
		37 ± 8 (weak)	§

*p < 0.01 vs. controls; †p < 0.01 vs. group A; ‡p < 0.01 vs. strong beat at 120 beats/min; §p < 0.01 vs. baseline; ‖p < 0.05 vs. group A; ¶p < 0.05 vs. controls.
LV dP/dt_{max} = maximal first derivate of left ventricular pressure; LVEDP = left ventricular end-diastolic pressure; LVPSP = left ventricular peak systolic pressure; $T_{1/2}$ = pressure half-time.

myocardial biopsy specimens was decreased in IDCM patients with pacing-induced mechanical alternans compared with that in those without it.

Despite recent improvements in the medical management of patients with IDCM, the overall prognosis of such individuals remains poor, with heart transplantation often being the only lifesaving therapeutic option (1,2,6). Even in patients with mild-to-moderate IDCM, sudden death occasionally occurs or hospitalization is needed for worsening heart failure. It has been difficult to predict such outcomes, however. Although several studies have attempted to identify prognostic factors for a poor outcome in patients with IDCM, none has revealed a factor proven to predict unequivocally the risk of cardiac events. Our present study is thus the first to show that the occurrence of pacing-induced mechanical alternans is a potential independent clinical predictor of cardiac events in patients with mild-to-moderate IDCM in sinus rhythm.

Pacing-induced mechanical alternans. We have shown that the amount of SERCA2 mRNA in LV endomyocardial biopsy specimens was decreased in IDCM patients with pacing-induced mechanical alternans compared with that in such patients without pacing-induced mechanical alternans, whereas the amount of ryanodine receptor 2 mRNA was significantly reduced in both patient groups compared with that in the control group. Because of the difficulty in obtaining appropriate specimens, few studies have investigated the cellular mechanism of mechanical alternans in the intact human heart. A reduction in the amounts of both SERCA2 and ryanodine receptor 2 mRNAs was previously described in humans with end-stage dilated cardiomyopathy at the time of heart transplantation (21,22).

Table 3. RT-PCR Analysis of the Abundance of Ca^{2+}-Handling Protein mRNAs (Normalized by the Amount of GAPDH mRNA) in Endomyocardial Biopsy Specimens

mRNA Ratio	Controls	Group A	Group B
SERCA2/GAPDH	1.24 ± 0.18	0.50 ± 0.12*	0.30 ± 0.13*†
Phospholamban/GAPDH	2.01 ± 0.69	2.13 ± 0.80	1.84 ± 0.19
Ryanodine receptor 2/GAPDH	1.45 ± 0.26	0.48 ± 0.16*	0.54 ± 0.34*
Calsequestrin/GAPDH	2.26 ± 1.75	1.61 ± 0.89	1.61 ± 1.25
Na^+-Ca^{2+} exchanger/GAPDH	2.68 ± 2.29	0.99 ± 0.84	1.37 ± 1.02
SERCA2/Na^+-Ca^{2+} exchanger	0.87 ± 0.65	1.20 ± 1.25	0.30 ± 0.20

*p < 0.05 vs. controls; †p < 0.05 vs. group A.
GAPDH = glyceraldehyde-3-phosphate dehydrogenase; RT-PCR = reverse transcription-polymerase chain reaction; SERCA2 = sarcoplasmic reticulum Ca^{2+}-ATPase.

Table 4. Univariate and Multivariate Predictors of Cardiac Events in IDCM Patients

	Univariate Analysis			Multivariate Analysis	
	Event-Free Group (n = 24)	Cardiac-Event Group (n = 10)	p Value	OR (95% CI)	p Value
Group A/group B	19/5	2/8	**0.004**	6.18 (1.31–29.2)	0.021
Age (yrs)	47 ± 13	52 ± 12	0.366		
Gender (M/F)	22/2	7/3	0.276		
LV end-diastolic dimension (mm)	63 ± 10	66 ± 7	0.290		
LV end-systolic dimension (mm)	51 ± 10	56 ± 7	0.139		
LV end-diastolic volume (ml)	195 ± 95	224 ± 97	0.442		
LV end-systolic volume (ml)	129 ± 79	161 ± 81	0.295		
LVEF (%)	38 ± 9	31 ± 7	**0.032**		
PAWP (mm Hg)	10 ± 6	18 ± 10	0.077		
Cardiac index (l min^{-1} m^{-2})	3.04 ± 0.66	2.57 ± 0.74	0.143		
Plasma BNP (pg/ml)	75 ± 78	238 ± 217	0.131		
Heart rate (beats/min)	74 ± 14	91 ± 19	**0.005**		
LV peak-systolic pressure (mm Hg)	121 ± 16	112 ± 22	0.147		
LV end-diastolic pressure (mm Hg)	11 ± 7	18 ± 10	**0.021**		
LVEDP/cardiac index (mm Hg min m^2 l^{-1})	3.83 ± 2.99	7.91 ± 5.32	**0.043**		
LV dP/dt_{max} (mm Hg/s)	1,266 ± 256	1,103 ± 208	0.083		
Peak change in LV dP/dt_{max} (%)	110 ± 11	112 ± 8	0.727		
$T_{1/2}$ (ms)	40 ± 8	43 ± 9	0.401		

Significant p values are shown in **bold** for univariate analysis.
CI = confidence interval; LVEDP = left ventricular end-diastolic pressure; OR = odds ratio; PAWP = pulmonary arterial wedge pressure. Other abbreviations as in Table 1.

Whether abnormal expression of the SERCA2 gene is responsible for mechanical alternans remains unclear. The presence of a delay between the uptake of Ca^{2+} into the sarcoplasmic reticulum and its subsequent release has been proposed to account for mechanical alternans (23–25). Our mRNA measurements do not directly reflect the Ca^{2+} uptake and Ca^{2+} release activities of sarcoplasmic reticulum in the myocardium. However, our data suggest that a decrease in the abundance of mRNAs for proteins that mediate Ca^{2+} uptake (SERCA2) or Ca^{2+} release (ryanodine receptor 2) might result in a reduction in the relative number of excitation-contraction coupling sites and in consequent dysregulation of Ca^{2+} handling by the sarcoplasmic reticulum in the failing myocardium. Such abnormal Ca^{2+} handling might substantially alter the force-frequency relation and myocardial performance.

Comparison with previous studies. Outcome can be improved in high-risk patients with CHF by treatment intensification and home-based interventions (7,26). However, there is currently no simple clinical criterion or score for predicting short-term outcome after discharge and thus for identifying patients for whom extra caution is required.

Plasma BNP level has been suggested to be a strong, independent predictor of cardiac events and sudden death in patients with CHF (27,28). A high plasma concentration of BNP before discharge was reported to be a powerful, independent marker of death or readmission in patients with decompensated CHF (7,29,30); BNP is thus now widely used as a clinical marker for differential diagnosis and management of heart failure. Patients with plasma BNP levels that do not correlate with the severity of their heart failure are encountered not infrequently, however. Several studies have suggested that BNP is substantially less accurate for detection of milder degrees of systolic dysfunction (10), which are more common than are severe forms but are also associated with increased risk. Additional studies are needed to define optimal therapy for mild asymptomatic LV systolic dysfunction (31).

Left ventricular ejection fraction has also been suggested as an independent prognostic factor (27,32,33). An LVEF of <20% was thus found to be associated with a one-year mortality of 30% in patients with dilated cardiomyopathy (4). However, other studies either did not support this finding (34,35) or showed that LVEF was less predictive than were other parameters such as transmitral inflow characteristics

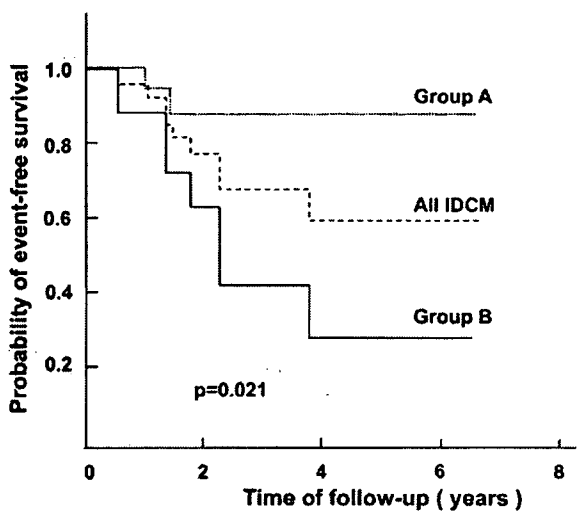

Figure 2. Cumulative probability of event-free survival calculated by the Kaplan-Meier method for all idiopathic dilated cardiomyopathy patients and patient groups A and B. The probability of event-free survival in group A was significantly greater than that in group B by the log-rank test (p = 0.021).

(5). A limitation of these markers, however, is their load dependence, which may confound accurate assessment of LV systolic or diastolic function and limit their predictive value (36).

The patients in our study were ambulatory, had a mean LVEF of 35%, and were in sinus rhythm. They were all of New York Heart Association functional class I or II, whereas most previous studies have been based on patients of class III or IV. In addition, most previous studies have included patients with atrial fibrillation. The presence of atrial fibrillation with heart failure has been shown to be independently associated with an increased risk for mortality (16).

Our prospective study constitutes the first demonstration that the occurrence of pacing-induced mechanical alternans is a potentially important and independent prognostic predictor in clinically stable and ambulatory patients with mild-to-moderate IDCM in sinus rhythm. Our results support the notion that assessment of contractile reserve and of responses to physiological stress in the myopathic heart provides important prognostic and pathophysiological insight over and above that derived under baseline conditions. For patients with IDCM, especially those in whom cardiac catheterization is performed for diagnosis, examination for the occurrence of pacing-induced mechanical alternans may thus provide prognostic information in addition to that based on LVEF or plasma BNP concentration.

Clinical implications and study limitations. The prevalence of cardiac events or cardiac death was higher in the patients with pacing-induced mechanical alternans than in those without it in the present study. Our results should therefore facilitate the clinical identification of patients with an increased mortality and morbidity risk, as well as prove helpful in the design of future trials examining mortality in individuals with mild-to-moderate IDCM. Assessment of pacing-induced mechanical alternans in addition to routine clinical evaluation in patients with mild-to-moderate IDCM may thus contribute to stratification of patients into low- or high-risk groups.

The identification of pacing-induced mechanical alternans requires an invasive examination. This condition is therefore not amenable to repeated assessment over time, possibly representing a limitation of its prognostic utility. The small number of patients enrolled in the present study and the limited number of variables tested for prognostic merit also represent limitations to the generalizability of its findings. Further studies with larger numbers of subjects will thus be needed to confirm our present results.

Conclusions. The occurrence of pacing-induced mechanical alternans was demonstrated to be a potentially useful clinical predictor of poor prognosis in patients with mild-to-moderate IDCM in sinus rhythm. The myocardial abundance of SERCA2 mRNA was decreased in patients with pacing-induced mechanical alternans compared with that in those without it. Whether these findings will also hold for patients with more severe heart failure requires further investigation.

Reprint requests and correspondence: Dr. Mitsuhiro Yokota, Department of Cardiovascular Genome Science, Nagoya University School of Medicine, 65 Tsurumai-cho, Showa-ku, Nagoya 466-8550, Japan. E-mail: myokota@med.nagoya-u.ac.jp.

REFERENCES

1. Dec GW, Fuster V. Idiopathic dilated cardiomyopathy. N Engl J Med 1994;331:1564–75.
2. Stevenson LW, Fowler MB, Schreder JS, et al. Poor survival of patients with idiopathic dilated cardiomyopathy considered too well for transplantation. Am J Med 1987;83:871–6.
3. Cohn JN, Archibald DG, Ziesche S, et al. Effect of vasodilator therapy on mortality in chronic congestive heart failure. N Engl J Med 1986;314:1547–52.
4. Keogh AM, Freund J, Baron DW, Hickie JB. Timing of cardiac transplantation in idiopathic dilated cardiomyopathy. Am J Cardiol 1988;61:418–22.
5. Pinamonti B, Lenarda AD, Sinagra G, et al. Restrictive left ventricular filling pattern in dilated cardiomyopathy assessed by Doppler echocardiography: clinical echocardiographic and hemodynamic correlation and prognostic implications. The Heart Muscle Disease study group. J Am Coll Cardiol 1993;22:808–15.
6. Kim S, Izawa H, Sobue T, et al. Prognostic value of mechanical efficiency in ambulatory patients with idiopathic dilated cardiomyopathy in sinus rhythm. J Am Coll Cardiol 2002;39:1264–8.
7. Logeart D, Thabut G, Jourdain P, et al. Predischarge B-type natriuretic peptide assay for identifying patients at high risk of re-admission after decompensated heart failure. J Am Coll Cardiol 2004;43:635–41.
8. Cheng V, Kazanagra R, Garcia A, et al. A rapid bedside test for B-type natriuretic peptide predicts treatment outcomes in patients admitted with decompensated heart failure. J Am Coll Cardiol 2001;37:386–91.
9. Vanderheyden M, Goethal M, Verstreken S, et al. Wall stress modulates brain natriuretic peptide production in pressure overload cardiomyopathy. J Am Coll Cardiol 2004;44:2349–54.
10. Redfield MM, Rodeheffer RJ, Jacobsen SJ, et al. Plasma brain natriuretic peptide to detect preclinical ventricular systolic or diastolic dysfunction. A community-based study. Circulation 2004; 109:3176–81.
11. Surawicz B, Fisch C. Cardiac alternans: diverse mechanisms and clinical manifestations. J Am Coll Cardiol 1992;20:483–99.
12. Lab MJ, Seed WA. Pulsus alternans. Cardiovasc Res 1993;27:1407–12.
13. Euler DE. Cardiac alternans: mechanism and pathophysiological significance. Cardiovasc Res 1999;42:583–90.
14. Kodama M, Kato K, Hirono S, et al. Mechanical alternans in patients with chronic heart failure. J Card Fail 2001;7:138–45.
15. Ryan JM, Schieve JF, Hull HB, et al. Experiences with pulsus alternans. Ventricular alternation and the stage of heart failure. Circulation 1956;14:1099–103.
16. Dries DL, Exner DV, Gersh BJ, et al. Atrial fibrillation is associated with an increased risk for mortality and heart failure progression in patients with asymptomatic and symptomatic left ventricular systolic dysfunction: a retrospective analysis of the SOLVD trials. J Am Coll Cardiol 1998;32:695–703.
17. Clark DM, Plumb VJ, Epstein AE, et al. Hemodynamic effects of irregular sequence of ventricular cycle lengths during atrial fibrillation. J Am Coll Cardiol 1997;30:1039–45.
18. Report of the WHO/ISFC task force on the definition and classification of cardiomyopathy. Br Heart J 1980;44:672–3.
19. Mirsky I. Assessment of diastolic function: suggested methods and future considerations. Circulation 1984;69:836–41.
20. Somura F, Izawa H, Iwase M, et al. Reduced myocardial sarcoplasmic reticulum Ca^{2+}-ATPase mRNA expression and biphasic force-frequency relations in patients with hypertrophic cardiomyopathy. Circulation 2001;104:658–63.
21. Arai M, Alpert NR, Maclennan DH, et al. Alterations in sarcoplasmic reticulum gene expression in human heart failure. A possible mecha-

nism for alterations in systolic and diastolic properties of the failing myocardium. Circ Res 1993;72:463–9.
22. Beuve CS, Allen PD, Dambrin G, et al. Cardiac calcium release channel (ryanodine receptor) in control and cardiomyopathic human hearts: mRNA and protein contents are differentially regulated. J Mol Cell Cardiol 1997;29:1237–46.
23. Schmidt AG, Kadambi VJ, Ball N, et al. Cardiac-specific overexpression of calsequestrin results in left ventricular hypertrophy, depressed force-frequency relation and pulsus alternans in vivo. J Mol Cell Cardiol 2000;32:1735–44.
24. Lab MJ, Lee JA. Changes in intracellular calcium during mechanical alternans in isolated ferret ventricular muscle. Circ Res 1990; 66:585–95.
25. Kihara Y, Morgan JP. Abnormal Ca_i^{2+} handling is the primary cause of mechanical alternans: study in ferret ventricular muscles. Am J Physiol 1991;261:H1746–55.
26. Anand IS, Florea VG, Fisher L. Surrogate end points in heart failure. J Am Coll Cardiol 2002;39:1414–21.
27. Berger R, Huelsman M, Strecker K, et al. B-type natriuretic peptide predicts sudden death in patients with chronic heart failure. Circulation 2002;105:2392–7.
28. Troughton RW, Frampton CM, Yandle TG, et al. Treatment of heart failure guided by plasma aminoterminal brain natriuretic peptide (N-BNP) concentrations. Lancet 2000;355:1126–30.
29. Tsutamoto T, Wada A, Maeda K, et al. Attenuation of compensation of endogenous cardiac natriuretic peptide system in chronic heart failure: prognostic role of plasma brain natriuretic peptide concentration in patients with chronic symptomatic left ventricular dysfunction. Circulation 1997;96:509–16.
30. Maeda K, Tsutamoto T, Wada A, et al. High levels of plasma brain natriuretic peptide and interleukin-6 after optimized treatment for heart failure are independent risk factors for morbidity and mortality in patients with congestive heart failure. J Am Coll Cardiol 2000;36:1587–93.
31. Wang TJ, Evans JC, Benjamin EJ, et al. Natural history of asymptomatic left ventricular systolic dysfunction in the community. Circulation 2003;108:977–82.
32. Cintron G, Johnson G, Francis G, et al. Prognostic significance of serial changes in left ventricular ejection fraction in patients with congestive heart failure. Circulation 1993;87 Suppl VI:VI17–23.
33. Wong M, Stazewsky L, Latini R, et al. Severity of left ventricular remodeling defines outcomes and response to therapy in heart failure. J Am Coll Cardiol 2004;43:2022–7.
34. Wilson JR, Schwartz JS, Sutton MS, et al. Prognosis in severe heart failure: relation to hemodynamic measurements and ventricular ectopic activity. J Am Coll Cardiol 1983;2:403–10.
35. Kelly TL, Cremo R, Nielsen C, et al. Prediction of outcome in late-stage cardiomyopathy. Am Heart J 1990;119:1111–21.
36. Kolias TJ, Aaronson KD, Armstrong WF. Doppler-derived dP/dt and −dP/dt predict survival in congestive heart failure. J Am Coll Cardiol 2000;36:1594–9.

Eplerenone Attenuates Myocardial Fibrosis in the Angiotensin II-Induced Hypertensive Mouse: Involvement of Tenascin-C Induced by Aldosterone-Mediated Inflammation

Tomohiro Nishioka, MSc, Maiko Suzuki, MSc,* Katsuya Onishi, MD,† Nobuyuki Takakura, MD,‡ Hiroyasu Inada, MD,* Toshimichi Yoshida, MD,* Michiaki Hiroe, MD,§ and Kyoko Imanaka-Yoshida, MD**

Abstract: Tenascin-C is an extracellular matrix glycoprotein that is supposed to be a profibrotic molecule in various fibrogenic processes. To elucidate its significance for myocardial fibrosis in the hypertensive heart, we used a mouse model with infusion of angiotensin II and examined results by histology, immunohistochemistry, in situ hybridization, and quantitative real-time reverse transcriptase polymerase chain reaction (RT-PCR). Angiotensin II treatment elevated blood pressure and expression of tenascin-C by interstitial fibroblasts in perivascular fibrotic lesions, and angiotensin II infusion caused accumulation of macrophages. It also upregulated expression of collagen Iα2; IIIα1; and proinflammatory/profibrotic mediators including transforming growth factor beta (TGFβ), platelet-derived growth factor alpha (PDGF-A), PDGF-B, and PDGF-receptor α, but not IL-1β and PDGF-receptor β, in the myocardium. Treatment with an aldosterone receptor antagonist, eplerenone, significantly attenuated angiotensin II–induced fibrosis, expression of tenascin-C, and inflammatory changes without affecting the blood pressure level. In vitro, neither eplerenone nor aldosterone exerted any influence on tenascin-C expression of cardiac fibroblasts, whereas angiotensin II, TGF-β1, and PDGF significantly upregulated expression of tenascin-C. These results suggest that, in the angiotensin II–induced hypertensive mouse heart: (1) tenascin-C may be involved in the progression of cardiac fibrosis and (2) aldosterone may elicit inflammatory reactions in myocardium, which might, in turn, induce tenascin-C synthesis of fibroblasts through at least 2 pathways mediated by TGF-β and PDGF-A-B/PDGF-receptor α.

Received for publication December 24, 2006; accepted January 10, 2007.
From the *Department of Pathology and Matrix Biology; †Department of Laboratory Medicine, Mie University Graduate School of Medicine, Tsu; ‡Department for Signal Transduction Research Institute for Microbial Diseases, Osaka University, Suita; and §Department of Nephrology and Cardiology, International Medical Center of Japan, Tokyo, Japan.
Sources of Support: A grant-in-aid for scientific research (No. 17590725) from the Ministry of Education, Culture Sports, Science and Technology of Japan to K.I.-Y. A grant for Intractable Disease from the Ministry of Health, Labor and Welfare of Japan to K.I.-Y and M. H.
Reprints: Kyoko Imanaka-Yoshida, MD, PhD, Department of Pathology and Matrix Biology, Mie University Graduate School of Medicine, 2-174 Edobashi, Tsu, Mie 514-8507 Japan (e-mail: imanaka@doc.medic.mie-u.ac.jp).

Key Words: myocardial fibrosis, tenascin, aldosterone, angiotensin II, hypertension, inflammation

(*J Cardiovasc Pharmacol*™ 2007;49:261–268)

INTRODUCTION

Diastolic dysfunction in the hypertensive heart is an important clinical problem, partly as a result of the rigidity caused by myocardial fibrosis. Such fibrosis has been classified into replacement (secondary) and reactive (primary) types.[1,2] In replacement fibrosis, necrosis of myocytes elicits acute inflammation and myocardial dropout is subsequently replaced by collagen fibers. In contrast, reactive fibrosis is characteristically observed in pressure overloaded hearts, in which collagen fibers increase in perivascular regions without loss of cells and eventually extend among individual cardiomyocytes.[3] Recently, inflammation mediated by the renin–angiotensin II (Ang II)–aldosterone system, especially involvement of aldosterone, has received much attention as a trigger of reactive fibrosis[4–7]; however, the molecular pathways remain to be detailed.

Fibrotic lesions do not form by abrupt deposition of collagen molecules; they form through multiple steps of synthesis and degradation of various matrix proteins, including tenascin-C. Tenascin-C is an extracellular glycoprotein with strong bioactivity, transiently expressed during embryonic development, wound healing, and cancer invasion.[8–10] Accumulating evidence suggests that tenascin-C may be a key regulator in an early step of the fibrotic process in various tissue.[11–13] In the heart, tenascin-C is sparsely detected in normal adults but becomes expressed in the pathological myocardium closely associated with inflammation and tissue remodeling.[14–21] Based on this specific expression, we recently reported that tenascin-C can be a clinical marker for active inflammation[18,19] and ventricular remodeling.[21,22]

The aim of the present study was to clarify the involvement of tenascin-C in the progression of reactive fibrosis in the hypertensive heart and the regulatory mechanism of tenascin-C expression, focusing on the angiotensin II–aldosterone system. We used a mouse model of hypertensive cardiac

fibrosis with infusion of Ang II in which reactive fibrosis develops in perivascular regions of myocardium without necrosis of cardiomyocytes or scar formation. First, we examined histologic changes and gene expression of collagen and tenascin-C in the mouse myocardium with immunohistochemistry, in situ hybridization, and quantitative real-time reverse transcriptase-polymerase chain reaction (RT-PCR). Next, to study the involvement of aldosterone and inflammation in regulation of tenascin-C synthesis, the effect of an aldosterone receptor blocker, eplerenone, and expression of proinflammatory/fibrotic mediators, transforming growth factor beta (TGFβ), interleukin-1 beta (IL-1β), and platelet-derived growth factor alpha (PDGF) in the model mouse were examined. Furthermore, the direct effects of these factors on tenascin-C synthesis were studied using cultured cells.

MATERIALS AND METHODS

Animal Model

Female 7-week-old BALB/c mice were used. All (n = 95) were given 1% NaCl drinking water and assigned to 1 of the following 5 groups: (1) vehicle control mice (n = 25); (2) Ang II-treated mice (n = 20); (3) Ang II/eplerenone-treated mice (n = 20); (4) eplerenone-treated mice (n = 19); and (5) aldosterone-treated mice (n = 11). A microosmotic pump (model 1002; Durect Co, Cuperino, CA) containing 0.1 mL of the vehicle (0.9% NaCl: 99.7% acetic acid = 15:1), 2.83 mg/mL of Ang II (SIGMA, St. Louis, MO), or 1 mg/mL of aldosterone (ACROS ORGANICS, NJ) was subcutaneously inserted under the back skin of each mouse for treatment for 4 weeks. The approximate doses of Ang II and aldosterone administered were 560 and 200 ng/kg body weight/min, respectively. The microosmotic pumps were replaced every 2 weeks. Eplerenone (Pfizer, New York), an aldosterone receptor blocker, was orally administered in the diet at 1.67 g/kg chow (the estimated dose of eplerenone was 250 mg/kg body weight/day). Body weights and blood pressure were examined every week. Blood pressure measurements were performed with the BP-98A (Softron, Tokyo, Japan) tail cuff system while the animals were conscious. All experimental protocols conformed to international guidelines and were approved by the Mie University Animal Experiment and Care Committee.

Tissue Preparation

After the 4 week infusion treatment period, the hearts were excised, fixed in 4% paraformaldehyde, and embedded in paraffin. For histopathological analysis, sections were cut at 3 μm.

Immunohistochemistry

Immunostaining of tissue sections was performed as previously described.[16] In brief, after treatment with pepsin for 10 minutes or heating in an autoclave for antigen retrieval, sections were incubated with either an antitenascin-C polyclonal rabbit antibody,[16] an anti-Mac-3 rat monoclonal antibody (Pharmingen, San Diego, CA; working dilution 1:10) for identification of macrophages, an anti-PDGF-A polyclonal rabbit antibody (Santa Cruz Biotechnology, Santa Cruz, CA; working dilution 1:20), an anti-PDGF-B polyclonal rabbit antibody (Santa Cruz Biotechnology, Santa Cruz, CA; working dilution 1:20), a rat monoclonal antimurine PDGFR-α antibody (Clone APA5),[23] or a rat monoclonal antimurine PDGF receptor-β antibody (Clone APB5).[24] Three independent fields in perivascular regions of myocardium from each mouse were examined under a 20× objective lens, and Mac-3-positive cells, PDGF-A, and PDGF-B positive cells were counted.

IMAGE ANALYSIS

Sirius red-stained slides were used to quantify myocardial collagen with an optical microscope (BH2, Olympus, Tokyo, Japan). Three independent perivascular fields from each mouse were visualized under a 20× objective lens and photographed with a Fujix Digital Camera HC 300Z/OL (Olympus). The images were analyzed using NIH Image, and percentage areas of perivascular fibrosis were calculated.

Quantitative Real-Time RT-PCR

Total RNA was extracted from fresh mouse left-ventricular tissues using ISOGEN (NipponGene, Toyama, Japan), and single-strand complementary DNA (cDNA) synthesis was performed by oligo $(dT)_{15}$ priming from 1 mg aliquots in a final volume of 20 mL with a single-strand cDNA synthesis kit for RT-PCR (Roche Diagnostics, Germany) according to the manufacturer's instructions. Quantitative analysis of target messenger RNA (mRNA) expression was performed with the TaqMan real-time RT-PCR and a relative standard curve method using Light Cycler Software Ver. 3.5 (Roche). The GAPDH mRNA level was quantified as an internal control. The primers and probes for mice are listed in Table 1.

In Situ Hybridization

Preparation of digoxigenin (DIG)-labeled mouse tenascin-C cRNA probes and *in situ* hybridization were performed as previously described.[16]

Cell Cultures

Cardiac fibroblasts were obtained from ventricles of Balb/c mice and grown in Iscove's modified Dulbecco's media (IMDM) with 10% fetal bovine serum as previously described.[20] Experiments were performed on secondary cultures. Cells (3×10^5 cells/well) were plated in MULTI-WELL 6-well plates (Becton Dickinson, Franklin Lakes, NJ) for 48 hours in serum-free IMDM media, then treated with Ang II (0 to 10^{-5} mol/L), aldosterone (0 to 10^{-6} mol/L), IL-1β (R&D Systems, Oxon, UK; 0 to 30 ng/mL), TGF-β1 (Roche Diagnostics; 0 to 10 ng/mL), or PDGF-BB (R&D Systems; 0 to 100 ng/mL) for 6 hours. Some cells were pretreated with eplerenone (10^{-8}, 10^{-7}, 10^{-6} mol/L) for 1 hour and then stimulated with Ang II (10^{-7} mol/L). To assess the combined effects of cotreatment with Ang II and aldosterone, cardiac fibroblasts were pretreated with aldosterone (10^{-6} mol/L) for 6 hours and then incubated with Ang II (10^{-7} mol/L) for 6 hours. Total RNA was isolated using ISOGEN, and the relative tenascin-C mRNA levels were determined by quantitative real-time RT-PCR.

TABLE 1. Oligonucleotide Primers and Probes Used for Real-Time RT-PCR

Gene	Primers and Probe Sequence	Product Size
Tenascin-C		
Forward	5′-AAGAATTTTGGCTTGGACTGGAT-3′	69
Backward	5′-GGTCCACCCGGAGCTCATA-3′	
Probe	5′-ACCTGAGCAAAATCACAGCCCAAGGG-3′	
Collagen Iα2		
Forward	5′-CAACCTGGACGCCATCAAG-3′	69
Backward	5′-CAGACGGCTGAGTAGGGAACA-3′	
Probe	5′-CCCAACCTGTAAACACCCCAGCGAAG-3′	
Collagen IIIα1		
Forward	5′-GGTGGTTTTCAGTTCAGCTATGG-3′	86
Backward	5′-CTGGAAAGAAGTCTGAGGAATGC-3′	
Probe	5′-TTCCTGAAGATGTCGTTGATGTGCAGCT-3′	
TGF-β1		
Forward	5′-TGGAGCTGGTGAAACGGAAGC-3′	400
Backward	5′-GTAGAGTTCCACCTGTTGCTCCACA -3′	
Probe	5′-CCGCGTGCTAATGGTGGACCGCAACAA -3′	
IL-1β		
Forward	5′-CAACCAACAAGTGATATTCTCCATG-3′	122
Backward	5′-GATCCACACTCTCCAGCTGC-3′	
Probe	5′-CTGTGTAATGAAAGACGGCACACCCACC-3′	
GAPDH		
Forward	5′-ATGGCCTTCCGTGTTTCCTAC-3′	85
Backward	5′-TGATGTCATCATACTTGGCAGG-3′	
Probe	5′-ATCCGTTGTGGATCTGACATGCCG-3′	

GAPDH, glyceraldehyde-3-phosphate dehydrogenase.

Statistical Analysis

All data are expressed as means ± standard deviations (SDs). Numeric data were statistically evaluated by 1-way analysis of variance, followed by the Tukey-Kramer method for multiple comparisons. A P value less than 0.05 was considered to be statistically significant.

RESULTS

Systolic Blood Pressure and Body Weight

Blood pressure was elevated within 1 week after the onset of Ang II treatment and remained significantly increased compared with that of the control mice for up to 4 weeks (Fig. 1A). No significant difference was observed between Ang II-treated and Ang II/eplerenone-treated groups. Blood pressure remained normal in vehicle-control, aldosterone-receiving, and eplerenone-alone mice. Increase in body weight was similar in all experimental groups during the study, and no statistically significant intergroup differences were observed at any time (Fig. 1B).

Myocardial Fibrosis and Expression of Tenascin-C

In Ang II-treated and aldosterone-treated mice, the volume of perivascular collagen fibers in myocardium was clearly increased, extending into spaces between individual myocytes. Eplerenone treatment almost completely abolished Ang II-induced perivascular fibrosis, and aldosterone treatment induced fibrotic changes (Fig. 2A). Necrosis of cardiomyocytes and scar formation were not found in our models.

Cardiac expression of tenascin-C was immunohistochemically detected in perivascular regions in Ang II-treated mice myocardium where collagen fibers had accumulated, whereas no immunostaining was observed in the control mice. Eplerenone reduced the tenascin-C expression induced by Ang II treatment, and aldosterone treatment induced tenascin-C expression (Fig. 2B).

In situ hybridization analysis for tenascin-C mRNA in Ang II-treated mice demonstrated signals in interstitial fibroblasts residing around the vascular tunica adventitia (Fig. 2C, D). Vascular endothelial cells, vascular smooth muscle cells, and cardiomyocytes were negative for tenascin-C mRNA.

Quantitative analysis of percentage fibrotic areas (Fig. 2E) confirmed a significant increase in Ang II-treated (12.9 ± 2.5%, $P < 0.001$) and aldosterone-treated (7.2 ± 2.0%, $P < 0.001$) mice compared with control mice (3.2 ± 0.9%). Fibrotic areas in eplerenone/Ang II mice were significantly attenuated (4.3 ± 1.8%, $P < 0.001$) as compared with Ang II-alone. Real-time RT-PCR analysis (Fig. 2F) showed that both Ang II and aldosterone significantly upregulated the mRNA levels for collagen type Iα2 (2.6 ± 1.0 and 1.8 ± 0.3-fold, $P < 0.01$, respectively) and for IIIα1 (3.2 ± 2.1-fold, $P < 0.05$ and 2.8 ± 0.4-fold, $P < 0.001$, respectively) when compared with the control mice (1.0 ± 0.4 and 1.0 ± 0.3-fold, respectively). Eplerenone treatment significantly reduced this upregulation of collagen Iα2 and IIIα1

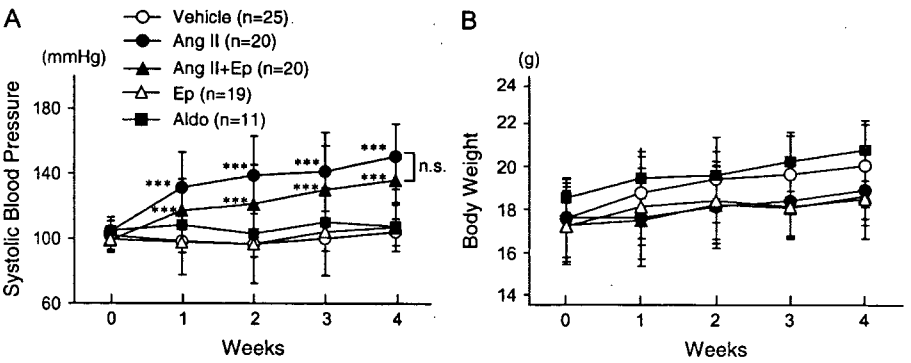

FIGURE 1. Systolic blood pressure (A) and body weights (B) for each group of mice. Values are means ± SD. Vehicle, vehicle control mice; Ang II, angiotensin II-treated mice; Ang II + Ep, Ang II/eplerenone-treated mice; Ep, eplerenone-treated mice; Aldo, aldosterone-treated mice. ***$P < 0.001$ vs vehicle control mice.